# The Response of Northern Hemisphere Snow Cover to a Changing Climate*

ROSS D. BROWN

*Climate Research Division, Environment Canada at Ouranos Inc., Montréal, Québec, Canada*

PHILIP W. MOTE

*Climate Impacts Group, CSES, JISAO, University of Washington, Seattle, Washington*

(Manuscript received 5 June 2008, in final form 14 October 2008)

ABSTRACT

A snowpack model sensitivity study, observed changes of snow cover in the NOAA satellite dataset, and snow cover simulations from the Coupled Model Intercomparison Project phase 3 (CMIP3) multimodel dataset are used to provide new insights into the climate response of Northern Hemisphere (NH) snow cover. Under conditions of warming and increasing precipitation that characterizes both observed and projected climate change over much of the NH land area with seasonal snow cover, the sensitivity analysis indicated snow cover duration (SCD) was the snow cover variable exhibiting the strongest climate sensitivity, with sensitivity varying with climate regime and elevation. The highest snow cover–climate sensitivity was found in maritime climates with extensive winter snowfall—for example, the coastal mountains of western North America (NA). Analysis of trends in snow cover duration during the 1966–2007 period of NOAA data showed the largest decreases were concentrated in a zone where seasonal mean air temperatures were in the range of −5° to +5°C that extended around the midlatitudinal coastal margins of the continents. These findings were echoed by the climate models that showed earlier and more widespread decreases in SCD than annual maximum snow water equivalent (SWEmax), with the zone of earliest significant decrease located over the maritime margins of NA and western Europe. The lowest SCD–climate sensitivity was observed in continental interior climates with relatively cold and dry winters, where precipitation plays a greater role in snow cover variability. The sensitivity analysis suggested a potentially complex elevation response of SCD and SWEmax to increasing temperature and precipitation in mountain regions as a result of nonlinear interactions between the duration of the snow season and snow accumulation rates.

## 1. Introduction

Snow cover represents a spatially and temporally integrated response to snowfall events, and the sequence of snowfall and melt events determines not just the quantity of water stored as snow but also snowpack condition (e.g., grain size and compaction), which in turn determines avalanche risk, energy required for melting, albedo of snow, and much more. Snowpack takes on special significance in mountain regions where snow stores enormous quantities of water, altering the ecologic and economic balance of regions far downstream by delaying the release of water months after precipitation events. Persistent changes in snow accumulation or melt can therefore have significant ecologic and economic consequences. Snow cover is also integrally linked with observed changes in global climate, especially for Northern Hemisphere (NH) land areas, through its role in modifying surface albedo. Observed monthly mean snow cover extent over the NH is strongly anticorrelated with air temperature, with the strongest relationships in the April–June period when extensive snow cover coincides with strong solar radiation (Déry and Brown 2007). Recently, Barnett et al. (2008) provided evidence of an anthropogenic signal in changes in snowpack and the hydrologic regime over the western United States.

Snow cover is anticipated to decrease in response to global warming, as snow cover formation and melt

* Joint Institute for the Study of the Atmosphere and Ocean Contribution Number 1584.

*Corresponding author address:* Ross Brown, Environment Canada at Ouranos Inc., 550 Sherbrooke St. West, 19th Fl., Montréal QC H3A 1B9, Canada.
E-mail: ross.brown@ec.gc.ca

DOI: 10.1175/2008JCLI2665.1

are closely related to a temperature threshold of 0°C. However, as first noted by Groisman et al. (1993) and more recently by Räisänen (2007), the snow cover response to global warming is complicated by projected increases in precipitation, particularly over high latitudes. The snow cover response to warming could therefore vary with latitude and elevation, with potential for increased accumulation in high latitudes and high elevations where increases in precipitation are sufficient to offset reductions in the length of the accumulation season. During the process of developing a synthesis of historical snow cover trends for the recent Intergovernmental Panel on Climate Change (IPCC) Fourth Assessment Report (Lemke et al. 2007), the authors were struck by the large variability in the published literature—for example, snow cover trends in the mountain regions of Europe are characterized by large regional and altitudinal variations (e.g., Vojtek et al. 2003; Scherrer et al. 2004; Brown and Petkova 2007); snow cover over North America (NA) has increased in the fall half of the year but decreased in the spring (Brown 2000); snow cover trends in China exhibit strong regional variations (e.g., Zhang et al. 2006; Qin et al. 2006; Zhao and Moore 2006; Changchun et al. 2007; Yang et al. 2007) despite widespread warming, glacier wasting, and permafrost thawing (Li et al. 2008); and snow depth trends over northern Eurasia show contrasting increases in the northeast and decreases in the west (Popova 2007).

Published trends in various snow cover variables from in situ data are summarized graphically in Fig. 1. Note that spatial sampling is highly irregular, and Fig. 1 is meant primarily as an inventory of published research (some mentioned above and some not) rather than an integrated global study. The panels distinguish types of snow quantities and in some cases seasons. Although each panel has some data points with positive trends and some with negative trends, the fraction of negative trends is larger for snow cover duration (SCD) than for midwinter snow depth and larger still for spring snow depth (SD) and snow water equivalent (SWE).

Two important factors contributing to this variability are the different periods used in the various studies and atmospheric circulation patterns such as North Atlantic Oscillation (NAO), which plays a role in the contrasting trends in Eurasian snow depth reported by Popova (2007). Other sources of variability are related to measurement issues (e.g., the spatial representativeness of point snow depth measurements, changes in measurement procedures, and others) and to the fact that the different variables used to monitor snow cover respond differently to a changing climate. For example, SD and SWE are more sensitive to changes in snowfall amount

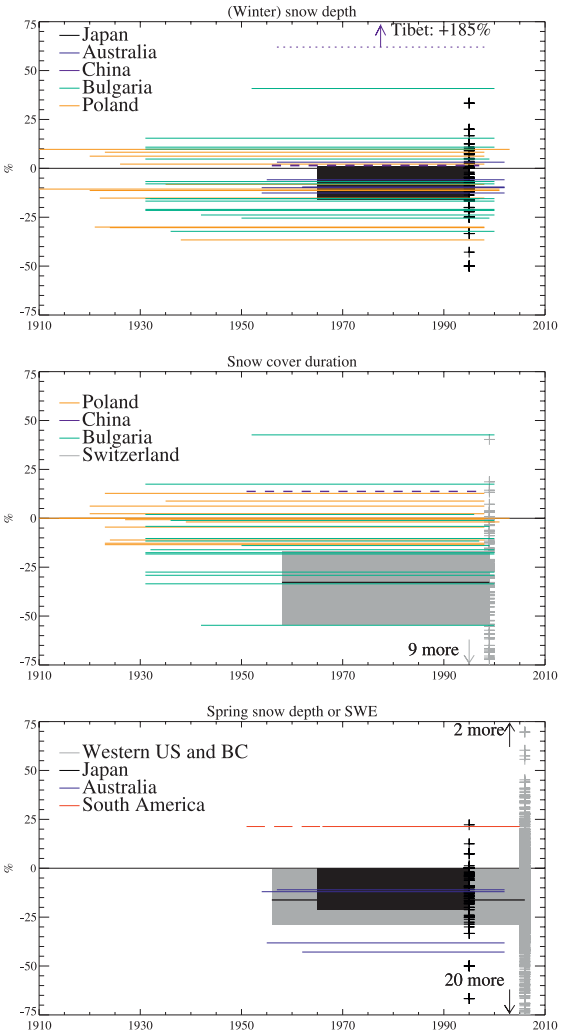


FIG. 1. Summary of published works describing trends in various snow quantities. The country shown is color-coded, and each line indicates the magnitude of the trend (*y* axis) and the duration (*x* axis). Dashed lines are estimated; thick lines are area averages; studies with large amounts of data (>50 points) are summarized with a colored box indicating the 25th and 75th percentiles, with a black line for the median; and pluses at the ending year indicate the trends at individual points. (top) Snow depth, which is computed as January–February, average for Japan (Ishizaka 2004), annual average for northwest China and Tibet (Qin et al. 2006); and maximum annual value for the four Australian stations (Hennessy et al. 2003), Bulgaria (Brown and Petkova 2007), and Poland (Falarz 2004). (middle) Annual snow cover duration for northwest China, Bulgaria, and Poland; and winter (December–February) duration for Switzerland (Scherrer et al. 2004). Note that nine Swiss stations had trends less than −75%, beyond the range of the plot. (bottom) SWE on 1 Apr for 11 western states and British Columbia (Mote 2006; note that 22 states/province lie beyond the range of the plot), March SD for Japan, 1 Sep SD for Australia, and an average of 6 snow courses (maximum annual SWE, usually in September) in Argentina and Chile (Masiokas et al. 2006); before 1966, only two to five snow courses were available, so the average is shown as a dashed line.

than snow-covered area (SCA) or SCD, which are closely controlled by air temperatures at the start and end of the snow cover season. SCA and SCD are also more closely linked to albedo feedbacks, which are stronger during the spring period (Groisman et al. 1993; Déry and Brown 2007) and over mountain regions (Giorgi et al. 1997; Fyfe and Flato 1999). The response of snow to climate change in mountain regions is further complicated by vertical gradients in temperature and precipitation. Typically, the largest relative changes are observed at lower elevations (e.g., Laternser and Schneebeli 2003; Scherrer et al. 2004; Mote et al. 2005; Mote 2006). However, there is evidence at some higher elevation sites of increased peak snow accumulation (e.g., Vojtek et al. 2003; Mote et al. 2005; Regonda et al. 2005) in response to increasing precipitation (Zhang et al. 2007).

The main purpose of this paper is to attempt to make some order out of the reported changes by placing observations of twentieth-century snow cover change into a framework of observed and expected changes. The expected changes were identified through (i) the sensitivity analysis, with a snowpack model to determine the response of different measures of snow to changes in temperature and precipitation; and (ii) the analysis of twentieth- and twenty-first-century changes in snow cover simulated by climate models to examine the spatial pattern and magnitude of snow cover response to warming. These were compared to observed changes in NH snow cover during the 1966–2007 period with the NOAA dataset (Robinson et al. 1993). The results from these analyses should provide some guidance on when snow-climate regions and elevation zones are likely to exhibit the earliest response to a changing climate and provide some context for interpreting published literature on changes in snow cover. This paper is organized as follows: a description of data sources used in the sensitivity analysis is provided in section 2; the methodologies for the snowpack model sensitivity analysis and the analyses of the NOAA dataset and the climate model output are presented in section 3, and the results are presented and discussed in section 4.

## 2. Data sources

### a. Climate station data

Daily maximum and minimum temperature and total precipitation data for the 1961–1990 period from four different sites in Canada (Table 1) were used in the snowpack sensitivity analysis. These sites come from four of the main snow-climate categories identified over the NH by Sturm et al. (1995): (i) the *maritime* class, characterized by relatively mild winter temperatures and high precipitation (Tahtsa Lake, British Columbia, henceforth referred to as TL); (ii) the *prairie* class, characterized by low precipitation, high winds, and variable winter temperatures (Saskatoon, Saskatchewan, henceforth referred to as SK); (iii) the *tundra* class, characterized by low precipitation, high winds, and cold temperatures (Resolute Bay, Northwest Territories, henceforth referred to as RB); and (iv) the *taiga* class, characterized by relatively cold temperatures and higher precipitation (Goose Bay, Newfoundland and Labrador, henceforth referred to as GB). Although the GB region is identified as taiga in the Sturm et al. (1995) classification, it is influenced by maritime air masses during winter and accumulates more snow than taiga sites located further inland. This site is still useful, however, as it is typical of the snow climate of central Quebec and Labrador, which has the largest annual snow accumulation in North America east of the cordillera. RB lies inside the November–May[1] −20°C isotherm, where climate models show an increase in maximum SWE in response to climate warming (Räisänen 2007; refer to Fig. 12). The relatively mild, heavy precipitation environment of TL in the British Columbia coastal mountains is typical of the Pacific Northwest snow climate, which has been shown to be particularly sensitive to climate warming (e.g., Hamlet et al. 2005; Bales et al. 2006). At this site, nearly 60% of the mean daily air temperatures below freezing are warmer than −5°C (Table 1), compared with ~25% for GB and SK and <15% for RB.

### b. NOAA satellite snow cover extent

National Oceanic and Atmospheric Administration satellite snow cover extent data were used to evaluate the snow cover climatologies of climate models from the Coupled Model Intercomparison Project phase 3 (CMIP3) multimodel dataset (Meehl et al. 2007) and to examine snow cover trends during the 1966–2007 period. The dataset is described in Robinson et al. (1993) and consists of weekly charts of the presence or absence of snow cover on a 190.5-km polar stereographic (PS) grid over the NH. The charting method changed in May 1999 with the introduction of the higher resolution (~25 km) daily interactive multisensor (IMS) snow cover product (Ramsay 1998). A pseudoweekly product has been derived from the IMS daily product by taking each Sunday map as representative of the previous week. This has resulted in obvious inconsistencies in snow

[1] Räisänen defined his −20°C isotherm for the November–March period, but the November–May period isotherm gives slightly better visual agreement with the zone where climate models indicate SWE will increase.

TABLE 1. Summary of climate stations used in the snow cover sensitivity analysis.

| Climate stations | Location | Snow-climate class[a] | Elevation (m) | Mean annual snowfall (cm)[b] | Mean winter temperature (°C)[b] | Freezing temperature warmer than −5°C[c] (%) |
|---|---|---|---|---|---|---|
| Resolute Bay | 74.7°N, 95.0°W | Tundra | 67 | 83.8 | −31.5 | 13.5 |
| Saskatoon | 52.2°N, 106.7°W | Prairie | 501 | 113.1 | −16.0 | 24.5 |
| Goose Bay | 53.3°N, 60.4°W | Taiga | 46 | 445.2 | −14.6 | 26.5 |
| Tahtsa Lake | 53.6°N, 127.7°W | Maritime | 863 | 1041.2 | −6.8 | 57.5 |

[a] From Sturm et al. (1995).
[b] From 1951 to 1980 published climate normals, Environment Canada.
[c] From observed daily climate data, 1961–90.

cover time series at 32 grid points in mountain and coastal areas, which were removed from the analysis. A homogeneity assessment of NOAA fall and spring snow cover duration with corresponding snow cover duration series from 133 stations across Canada indicated no evidence of a discontinuity in 1999 with the change in procedures, but there was evidence of a systematic improvement in the product with linear increases in the correlation between NOAA and corresponding surface observations in both the fall and spring snow seasons, and a statistically significant (0.05 level) reduction in the difference between NOAA and stations of −0.24 day $yr^{-1}$ in the spring period. This is likely related to the increasing frequency and resolution of satellite coverage over time and to the increasing skill of analysts and was most marked over mountain regions. There was no change in the NOAA–station difference in the fall season, which may reflect the more rapid nature of snow onset versus spring melt (i.e., less potential for obscuring cloud and patchy snow). This problem requires more detailed analysis with in situ data from other regions of the NH before corrections can be applied. However, it appears from the Canadian evaluation results that the effect of improvements in snow mapping over time is an order of magnitude smaller than the observed trends in SCD from surface observations, so this is unlikely to change conclusions about where snow cover is exhibiting the largest changes. Monthly snow cover duration data were obtained from Rutgers University, which contain the corrections recommended by Robinson et al. (1991) and the Rutgers weighting scheme (Robinson 1993) to correctly partition weekly charts into appropriate months. Trend analysis of snow cover duration was carried out for the snow year (August–July) and for the fall (August–January) and spring (February–July) halves of the snow year using the Mann–Kendall method.

### c. WCRP's CMIP3 multimodel dataset

Monthly snow cover and snow water equivalent output from models in the World Climate Research Programme's CMIP3 multimodel dataset (Meehl et al. 2007) were obtained to examine the simulated trends in twentieth-century snow cover and the projected changes in snow cover under the A2 scenario to determine the regions where snow cover signals first emerge. Models were only included if they had SWE or snow cover output for both the twentieth-century 20C3M simulation and the A2 emission scenario. Most modeling groups provided SWE output, but only about half the models had information on snow cover. SWE output was obtained from 14 models and snow cover output from 8 models (Table 2) through the Earth System Grid data portal (available online at ftp://ftp-esg.ucllnl.org). A number of these models are closely related to each other, but Räisänen (2007) found there could be substantial differences in climate between similar models. Although some models provided multiple simulations, distinguished only by different initial conditions, we only examine one simulation (''Run1'') per model, as not all models provided multiple runs.

Monthly snow cover fraction was multiplied by the number of days in a month to obtain estimates of annual and seasonal snow cover duration, as daily model output was not readily available for many of the models. Change in SWE was assessed by looking at the change in annual maximum monthly SWE during a snow year, which was defined as starting in August and ending in July. This takes account of potential shifts in the timing of peak SWE.

### d. Northern Hemisphere SWE climatology

It was not the purpose of this paper to carry out a detailed evaluation of SWE simulated by the CMIP3 models. However, it is important to have some idea of how well the models simulate SWE and to identify obvious problem areas if the models are to be used as guidance for interpreting current trends. A high-quality global SWE dataset does not exist for evaluating climate models. Brown et al. (2003) developed a daily SWE analysis for NA for the second phase of the Atmospheric Model Intercomparison Project (AMIP2)

TABLE 2. Summary of climate models used in this study.

| Model | Modeling Group | Global grid resolution (nlon × nlat) | Snow cover | SWE |
|---|---|---|---|---|
| CCSM3 | National Center for Atmospheric Research, United States | 256 × 128 | x | x |
| CGCM3.1 (T47) | Canadian Centre for Climate Modeling and Analysis, Canada | 96 × 48 | x | x |
| CNRM-CM3 | Météo France | 128 by 64 | | x |
| CSIRO Mk3.0 | CSIRO Atmospheric Research, Australia | 192 × 96 | x | x |
| CSIRO Mk3.5 | CSIRO Atmospheric Research, Australia | 192 × 96 | x | |
| ECHAM5 | Max Planck Institute for Meteorology, Germany | 192 × 96 | | x |
| ECHO-G | University of Bonn, Germany and Korean Meteorological Agency, Korea | 96 × 48 | | x |
| GFDL CM2.1 | Geophysical Fluid Dynamics Laboratory, United States | 144 × 90 | | x |
| GISS-ER | Goddard Institute for Space Studies, United States | 72 × 46 | x | x |
| HadCM3 | Hadley Centre for Climate Prediction and Research, United Kingdom | 96 × 73 | | x |
| HadGEM1 | Hadley Centre for Climate Prediction and Research, United Kingdom | 192 × 145 | | x |
| INM-CM3.0 | Institute for Numerical Mathematics, Russia | 72 × 45 | x | x |
| IPSL-CM4 | Institut Pierre Simon Laplace, France | 96 × 72 | | x |
| MIROC32 (medres) | Center for Climate System Research, Japan | 128 × 64 | x | x |
| MRI- CGCM2.3.2 | Meteorological Research Institute, Japan | 128 × 64 | x | x |

period (1979–97) from historical snow depth observations, but this effort has not been duplicated in Eurasia, where the historical data are spread across many countries and organizations. Roesch (2006) generated a global SWE climatology from the U.S. Air Force (USAF) snow depth climatology (Foster and Davy 1988), but Brown and Frei (2007) show that values of spatially averaged SWE over the NH are likely underestimated by about 50% (or 30 mm) in the spring as a result of shortcomings in the USAF dataset and the specification of snow densities that were too low.

The SWE climatology used in this study was derived from the daily global snow depth analysis generated by the Canadian Meteorological Centre (CMC) since March 1998 and described in Brasnett (1999). The daily snow depth analyses were converted to SWE by applying a snow density lookup table developed from analysis of Canadian historical snow course data (Meteorological Service of Canada 2000) for the six main snow climate classes defined by Sturm et al. (1995; Table 3). All six classes are found in Canada, allowing mean density information to be generalized to the rest of the NH using the 0.5° × 0.5° gridded version of the Sturm et al. (1995) classification (Liston and Sturm 1998). The use of a snow density climatology to estimate SWE is considered valid, because snow depth variability is the dominant factor driving spatial and temporal variability in SWE (Pomeroy and Gray 1995) and because snow density tends to follow the same seasonal evolution with relatively low interannual variability (Brown 2000). Mean annual maximum monthly SWE values during the 2001–06 period were interpolated to a 190.5-km NH PS grid for comparison with the climate models. This relatively short period was the longest period of overlap that could be obtained based on the availability of the observed and simulated data.

## 3. Methodology

### *a. Sensitivity analysis*

One of the main motivations for this paper was to examine the role of snow cover as a potential climate indicator. The question of which snow properties (e.g., snow cover duration, peak SWE, melt onset date, and others) are most appropriate for monitoring for climate change detection was first posed by Goodison and Walker (1993). Barry (1984) proposed that candidate climate monitoring indices should do the following:

- show high sensitivity to meteorological variables responding to greenhouse gas (GHG) forcing;
- have a short response time;
- have a high signal-to-noise ratio; and
- be consistently measured over an extended period of time.

The first three criteria were tested by carrying out a sensitivity analysis of snow cover simulated by the temperature–index snowpack model described in Brown et al. (2003). The model incorporates most of the temperature-dependent processes included in detailed physical models (e.g., partitioning of precipitation into solid and liquid fractions, melt from rain-on-snow events, specification of new snowfall density, snow aging, and snowmelt). Snowmelt is parameterized as a function of snow density following Kuusisto (1980) to simulate the effect of decreasing albedo on spring snowmelt rates. As a minimum, the model requires daily values of maximum

TABLE 3. Mean monthly snow density (kg $m^{-3}$) lookup table used to estimate SWE from snow depth based on Canadian snow course observations. The snow classes are those defined by Sturm et al. (1995).

| Month | Tundra | Taiga | Maritime | Ephemeral | Prairie | Alpine |
|---|---|---|---|---|---|---|
| October | 200.0 | 160.0 | 160.0 | 250.0 | 140.0 | 160.0 |
| November | 210.7 | 176.9 | 183.5 | 300.0 | 161.6 | 172.0 |
| December | 218.1 | 179.8 | 197.7 | 335.1 | 185.1 | 181.6 |
| January | 230.3 | 193.1 | 216.5 | 316.8 | 213.7 | 207.2 |
| February | 242.7 | 205.9 | 248.5 | 337.3 | 241.6 | 241.5 |
| March | 254.4 | 221.8 | 283.3 | 364.3 | 261.0 | 263.5 |
| April | 273.6 | 263.2 | 332.0 | 404.6 | 308.0 | 312.0 |
| May | 311.7 | 319.0 | 396.3 | 458.6 | 398.1 | 399.6 |
| June | 369.3 | 393.4 | 501.0 | 509.8 | 464.5 | 488.9 |

($T_{max}$) and minimum ($T_{min}$) temperature and daily total precipitation. For this study, the model was run at a 6-hourly time step to capture the diurnal cycle, with 6-hourly temperatures estimated from weighted values of $T_{max}$ and $T_{min}$ following Anderson (1973). The model assumed a temperature threshold of 0°C for rain/snow separation and a melt threshold temperature ($T_{melt}$) of −1°C based on an evaluation of the model at several sites across Canada by Brown et al. (2003). A melt threshold less than 0°C is physically realistic, since radiation melt can take place when air temperatures are below freezing. Kuusisto (1984) obtained $T_{melt}$ values of −1.3° and −1.2°C for open and forested sites, respectively, in Finland.

The choice of snow cover variables was based on key properties of a snowpack related to the timing of snow cover onset and melt and the amount of accumulated snow. The most commonly used snow cover properties in the literature are the first and last date of snow on the ground (e.g., Ye 2001); the first and last dates of continuous snow cover, which requires definition of depth and duration thresholds; the duration of snow on the ground, which may involve the setting of depth thresholds for in situ data (e.g., Brown 2000); and variables describing the amount of accumulated snow, such as mean, median, and maximum snow depth or SWE. For this study, the following snow cover parameters were selected and calculated for a snow year defined from 1 August to 31 July:

- first (JDfirst) and last (JDlast) dates of any snow on the ground;
- the start (JDstart) and end (JDend) dates of continuous snow cover defined as the first date with seven continuous days of SWE values ≥4 mm, and the first date with seven continuous days of SWE values <4 mm;
- the snow cover duration (days with SWE ≥2 mm) in the fall (SCD1) and spring (SCD2) halves of the snow cover season and during the entire snow year (SCDann);
- annual maximum SWE (SWEmax); and
- date of annual maximum SWE (JDmax).

Snow cover duration variables were set to missing once the snowpack persisted beyond the end of a snow year. Comparison of the coefficient of variation (CV), or relative dispersion, defined as the ratio of the standard deviation to the mean, for observed and simulated annual snow cover statistics during the 1961–90 period (Fig. 2) at sites from three different snow-climate regions in Canada revealed the snowpack model correctly captured the differences in CV between snow cover variables with the exception of JDmax, where the model simulated a lower interannual variability. This is likely linked to the model not having precise information on the solid/liquid fraction of precipitation. Realistic simulation of the CV is important for assessing changes computed with Eq. (1) (see below).

The snow cover sensitivity analysis was carried out over a temperature ($T$) and precipitation ($P$) change range of +4°C and +30%, which approximates the upper range of projected future changes over NH mid-to-high latitudes reported in the recent IPCC fourth assessment report (Christensen et al. 2007). Simulations were run using a 30-yr block of observed daily climate data (1961–90) to evaluate the significance of simulated changes following Eq. (1) below. Simulations were also carried out over 10 250-m elevation increments above the station elevation, assuming a mean lapse rate of −6.5°C $km^{-1}$ to investigate the effect of local changes in elevation on snow trends in the climate zones represented by each of the stations. Precipitation amounts were not adjusted for elevation.

The sensitivity of snow cover variables to changes in temperature and/or precipitation was assessed by computing the Student's $t$ statistic for a change in mean following Fyfe and Flato (1999):

$$(S_{fut} - S_{ref})/\sigma, \quad (1)$$

where $S_{ref}$ is the 30-yr snow cover variable mean for 1961–90, $S_{fut}$ is the 30-yr mean for changed $T$ and $P$, and $\sigma$ is the pooled standard deviation for the two 30-yr periods.

These sensitivity experiments or *incremental analogs* (Mearns et al. 2001) are easy to apply but contain some inherent weaknesses that must be acknowledged. First, they ignore local feedbacks in the warming response—for example, the snow–albedo feedback, which is stronger in the spring than in the fall (Groisman et al. 1994; Déry and Brown 2007). Second, they assume that the variance in temperature and precipitation does not change in

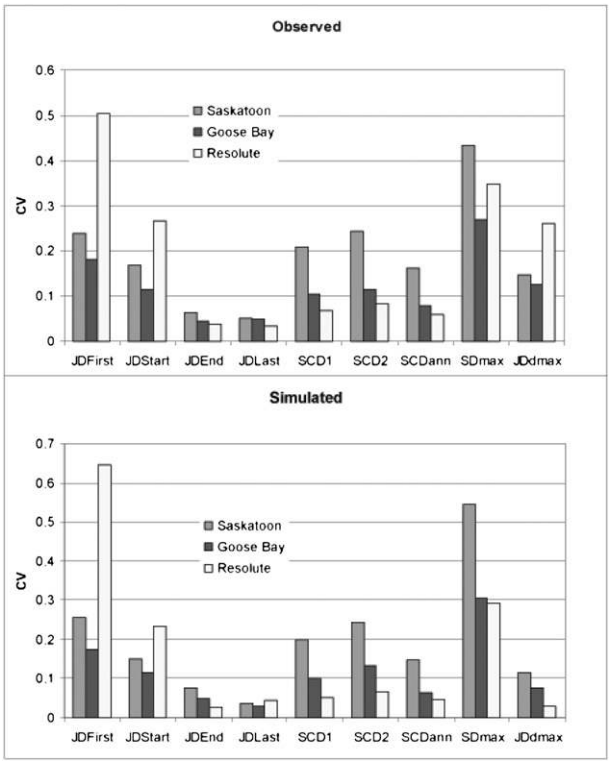


FIG. 2. The CV of annual snow cover variables computed from (a) observed and (b) simulated daily snow depth during the 1961–90 period at three of the sites used in the sensitivity analysis. There were insufficient snow depth observations at TL to compute snow cover statistics. Note that SDmax is used to define maximum accumulation in this comparison.

response to warming. Third, they assume that the seasonality of the precipitation regime remains unchanged and that all regions experience the same warming and increase in precipitation. However, it is argued that this approach is still useful, as it provides information on the *relative* sensitivity of the various snow cover variables in different climate regimes.

### b. Trend analysis of observed snow cover

The NOAA dataset was used to document observed trends in snow cover over the Northern Hemisphere land areas from 1966 to 2007. This period was characterized by statistically significant (0.05 level) warming in all months over NH midlatitudes based on analysis of the CRUtem3v dataset (Brohan et al. 2006) with fall and spring season warming of ~1.5°C, which accounts for a large fraction of the warming experienced since 1900. Trends in annual (SCDann) and seasonal (SCD1 and SCD2) snow cover duration during 1966–2007 were computed using the nonparametric Kendall's rank correlation (Sen 1968) and taking serial correlation into account following Zhang et al. (2000). The Kendall estimate is used instead of least squares, as it is less sensitive to nonnormally distributed variables and is less affected by extreme values or outliers in the series. A Monte Carlo method was used to estimate the confidence interval for the estimate slope and the 5% level of significance used to define statistically significant trends. Grid points were excluded from the analysis, where more than half the years had either zero snow cover or were completely snow covered (i.e., points where snow cover duration is strongly skewed) and the trend $Z$ statistic was plotted to give an indication of the relative strength of the changes in snow cover. It was not possible to make inferences about the statistical significance of the trends as a result of the likely presence of technological bias, which requires further work to document and correct.

### c. Climate model analysis

The purpose of the climate model analysis was to determine whether they showed any evidence of changes in snow cover during twentieth-century climate simulations and to identify the locations and snow variables where future changes may be first identified. The snow cover variables assessed were seasonal snow cover duration (SCD1, SCD2, and SCDann) and SWEmax. It was not possible to evaluate other snow variables (e.g., onset dates), as daily model output are not readily available for snow-related variables.

Snow cover changes were assessed over 30-yr averages using Eq. (1) to compute the $t$ statistics between a 30-yr period mean and the reference climate mean. The period 1970–99 was defined as the "current climate" reference for future climate changes, which were based on the A2 emission scenario. The 30-yr periods used for assessing future changes were 2010–39, 2040–69 and 2070–99. Twentieth-century changes were assessed with model output from 20C3M runs, with change computed between 1900–29 and 1970–99. The change statistics from the various models were interpolated to a common 190.5-km PS grid (the NOAA grid) using the nearest-neighbor method to summarize the results. The percent of models showing statistically significant changes of the same sign was also plotted on the common grid to obtain an indication of model consensus.

A brief evaluation was made of the models' ability to simulate the observed mean annual snow cover duration and annual maximum monthly SWE climatologies over the Northern Hemisphere, as this was not included in the IPCC model evaluation (Randall et al. 2007), and recent evaluations such as Roesch (2006) only looked at the mean seasonal cycle. Frei and Gong (2005) provided a preliminary evaluation of the CMIP3 models over North America and found significant between-model

variability, with most models underestimating mean continental snow-covered area.

Figure 3 compares the mean model annual SCD climatology for 1970–99 with the corresponding annual SCD climatology from the NOAA dataset with the fall and spring season difference fields presented in Fig. 4. The models do a reasonable job of simulating the mean spatial pattern of annual SCD in agreement with previous evaluations (Foster et al. 1996; Frei and Robinson 1998; Frei et al. 2003, 2005), with spatial correlation coefficients (not shown) ranging from 0.78 to 0.89 across the eight models. The mean model difference in annual SCD averaged over the NH was −5 days. The one area where the models performed poorly was the Tibetan Plateau, where annual SCD was overestimated by an average of more than 100 days. This problem was previously identified by Frei et al. (2003), who attribute this to systematic cold and wet biases in the models over the Tibetan Plateau that still exist in the CMIP3 models (Randall et al. 2007). The underestimation of snow cover over mountain regions in Fig. 4 (e.g., western cordillera of North America) is mainly related to the smoothed topography in most of the models. The spring and fall SCD differences are similar except for a tendency for the models to underestimate SCD in the spring over high latitudes. However, recent evidence from northern Canada indicates the NOAA dataset has a delayed spring melt response (Wang et al. 2005; Brown et al. 2007), which could account for some of this difference.

The SWE climatology comparison was carried out during the 2001–06 period, which was the longest period of overlap between the GCMs and the CMC-estimated SWE values (Fig. 5). The Goddard Institute for Space Studies (GISS) model was excluded from the model mean, as twenty-first-century data only started in 2004. Analysis of individual model spatial correlations and differences (not shown) yielded lower correlations than annual SCD, with little difference between the 13 models ($r$ = 0.60–0.67). The difference field results show that GCM-simulated SWEmax values are typically 40–80 mm higher over mid-to-high latitudes than those estimated from the CMC daily snow depth analyses, although this may be exaggerated, as the CMC SWE climatology appears to underestimate high-latitude SWE when compared to recent field observations (C. Derksen 2007, personal communication). This underestimate is likely related to the fact that the snow depth observations used in the CMC analysis tend to be taken in open locations that are more susceptible to wind scour and earlier snowmelt.

Apart from Frei et al. (2005), who reported positive SWE biases over northern Canada for AMIP2 AGCMs, previous evaluations of snow mass in GCMs (e.g., Roesch 2006) have tended to focus on continental-scale-averaged SWE, where spatial averaging reduces the importance of high-latitude positive SWE biases. For example, in Fig. 5, the mean SWE bias is only +15 mm when averaged over the NH snow-covered area. The high-latitude positive SWE bias is also linked in part to a tendency for the models' simulated precipitation to be about 15–20 cm yr$^{-1}$ more than satellite-derived observations over land areas north of ~40°N (see Fig. S8.10 in Randall et al. 2007), together with a slight cold bias (Randall et al. 2007). Räisänen (2007) found good agreement between climate model simulations of annual maximum monthly SWE and historical snow course data from the former Soviet Union (Fig. 1d of Räisänen 2007). However, his comparison was mainly confined to the region south of 60°N, and there were few observations over northeastern Russia, where Fig. 5 suggests the models overestimate annual maximum SWE.

## 4. Results

### a. Sensitivity analysis

Before proceeding with the presentation of the sensitivity results from the snowpack model, it is important to stress that the results should be interpreted in a relative sense because of the numerous site-related processes affecting snow cover that are not incorporated in the model (e.g., blowing snow, vegetation interactions, among others). This is also the case for the elevation change results that depend on local topography and local lapse rates, which can differ markedly from the assumed mean value of −6.5°C km$^{-1}$ used here. For example, Marshall et al. (2007) report mean daily lapse rates of −4.1°C km$^{-1}$ from Ellesmere Island in the Canadian Arctic. It should also be noted that investigation of the influence of elevation is carried out with respect to the local elevation of the station and is written as $\Delta Z$; thus, $\Delta Z$ = 2000 m refers to the estimated snow climate 2000 m above the surface where the data were collected. The purpose of this analysis is to determine how snow cover may vary with elevation in the four snow-climate regions represented by each station, some of which include terrain at altitudes 1000–2000 m higher than the station.

The $t$ statistics for simulated snow cover change in response to joint linear increases in air temperature and precipitation of +4°C and +30%, respectively, by small proportional increments, are plotted in Fig. 6 for $\Delta Z = 0$. The results show that snow cover responds very rapidly to warming, with locally significant reductions in snow cover duration emerging at TL, GB, and RB for an annual warming of 0.6°–0.8°C. In general, snow cover

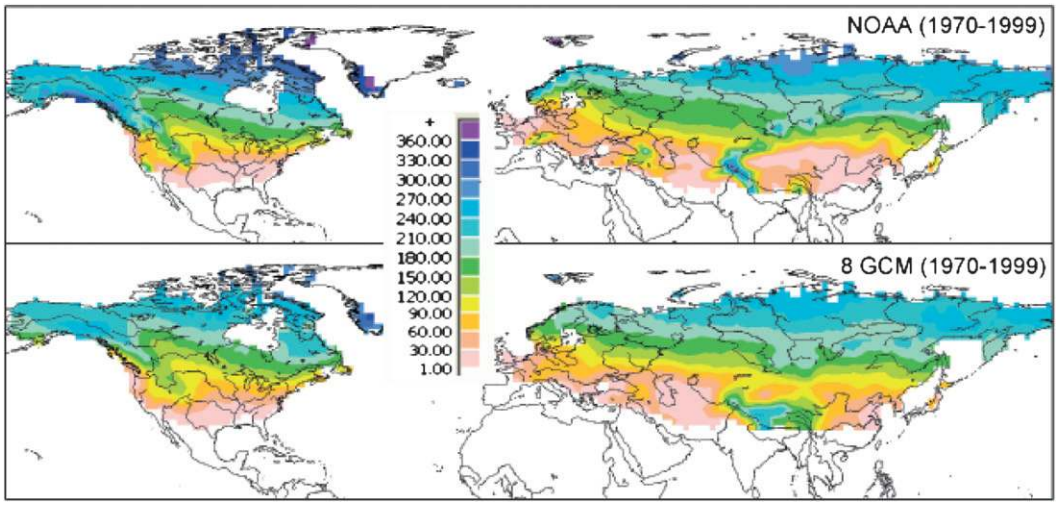


FIG. 3. Comparison of mean annual SCD (days) from the (top) NOAA weekly dataset and (bottom) eight GCM average.

duration variables, such as annual snow cover duration, showed greater sensitivity to warming than variables related to depth, such as SWEmax or JDMax. Averaged across all four sites, SCDann gave the largest change signal followed by JDLAST, SCD1, and SCD2. One of the reasons for this is that these snow cover variables tend to be less noisy than SWEmax, as evident from the CV for observed annual snow cover variables (Fig. 2).

TL exhibited the strongest temperature sensitivity of the four sites, with all nine snow cover variables displaying significant changes for a warming of only 1.5°C. The stronger sensitivity of snow cover and SWE to warming is related to the relatively warm, wet winter climate at TL (see Table 1), which means that small changes in temperature generate large changes in the fraction of precipitation falling as snow and the number of snowfall days. Indeed, for similar climates of western North America south of TL, Knowles et al. (2006) found large changes in the fraction of precipitation falling as snow, and Mote (2006) found a strong statistical connection between temperature variability and springtime SWE variability. SK displayed the lowest temperature sensitivity of the four sites, which seems counterintuitive, since one would expect shallow prairie snowpack to be sensitive to warming at the start and end of the snow season. However, this site tends to have a noisier

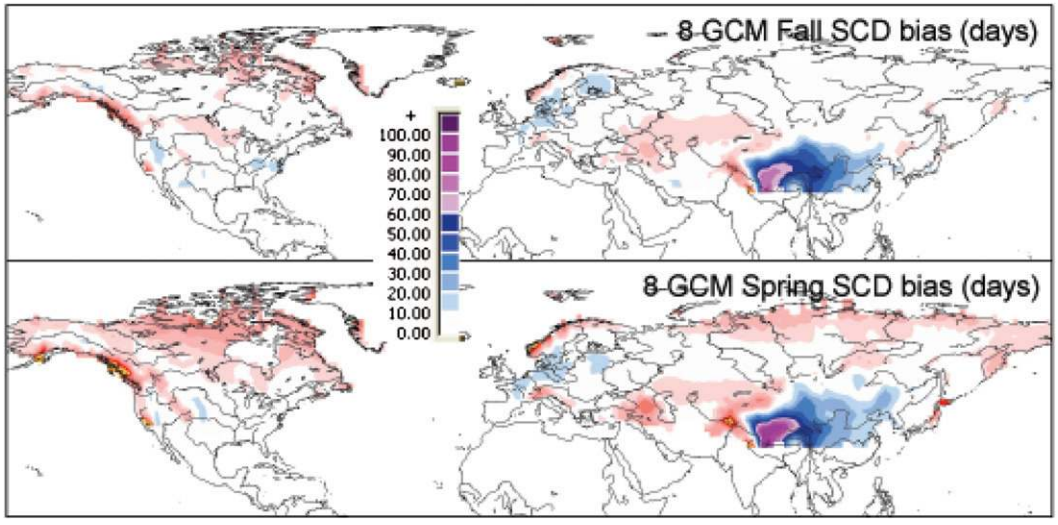


FIG. 4. Mean GCM bias in (top) fall and (bottom) spring SCD (days) compared to the NOAA weekly dataset, 1970–1999.

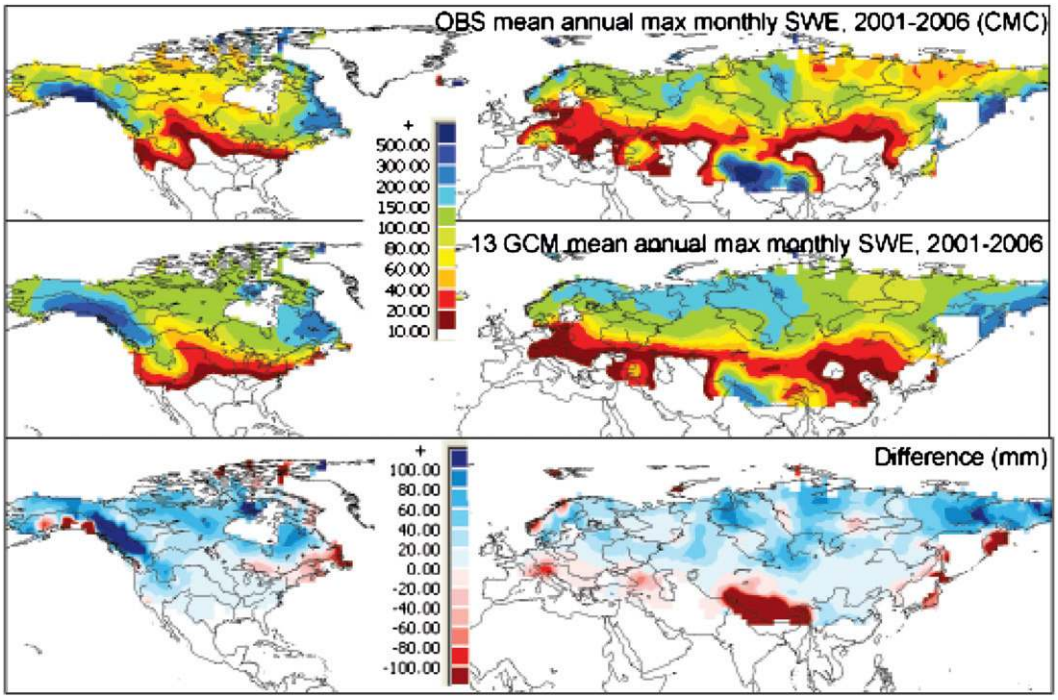


FIG. 5. Comparison of (middle) 13 GCM mean SWEmax (mm), with (top) estimated SWEmax from CMC daily snow depth analyses for 2001–06 and (bottom) mean model bias (mm).

snow cover climate than the other sites (see Fig. 2) and the temperature change signal is small, because the transition period of near-freezing temperature is half as long as TL and winter precipitation is an order of magnitude smaller (Table 1).

Comparison of sensitivity results with $P$ varied and $T$ held constant (not shown) indicated that increasing precipitation has only a small effect in delaying the snow cover change signal at all four stations, but a strong influence in delaying the onset of significant reductions in SWEmax, particularly at the two lower precipitation sites (RB and SK). The stronger sensitivity of SWEmax to precipitation changes in cold, dry environments may complicate the interpretation of snow trends in these climate regions. This appears to be the case in western China, where there is a wide range in reported snow cover trends (e.g., Qin et al. 2006).

An interesting result of the sensitivity analysis was the identification of significant shifts to earlier dates of maximum SWE (JDmax) *before* significant reductions in SWEmax emerged at three of the four sites. This result is partly due to the underestimation of interannual variability in JDmax by the snow model (Fig. 2). However, the observations also indicate there is less noise in the date of maximum accumulation than annual maximum depth, which suggests it may be a useful variable for climate monitoring.

The elevation response of snow cover to the warmer, wetter scenario evaluated in this study is shown in Fig. 7. Increases in SWEmax are only simulated over higher elevations where the warming influence is offset (Fig. 7a) with the height of the zero-change line ranging from $\Delta Z = 750$ m at SK to $\Delta Z = 1100$ m at TL. Increasing SWE at higher elevations has been documented over the western United States (Mote et al. 2005; Regonda et al. 2005) and the mountains of Slovakia (Vojtek et al. 2003). The elevation response of SWEmax involves nonlinear interactions between changing snow season length and changing snowfall amount and frequency. This nonlinear response can be expected to contribute to regional-scale variability in the elevation response of snow cover to climate change, which will be modified by local factors, such as lapse rate, aspect, and topography, among others. For example, Vojtek et al. (2003) estimated a zero-change elevation of 1800 m on north-facing slopes and 2300 m on south-facing slopes for snow cover change in Slovakian mountains during the 1920–2000 period.

TL exhibited the strongest elevation dependence and the strongest temperature sensitivity, which reached maximum values for SWEmax of $-150\,\text{mm}\,^{\circ}\text{C}^{-1}$ at $\Delta Z = 500$ m and SCDann of $-25$ days $^{\circ}\text{C}^{-1}$ at $\Delta Z = 250$ m (Fig. 7b). This is an order of magnitude higher than GB and almost two orders of magnitude higher than SK or RB, but it is

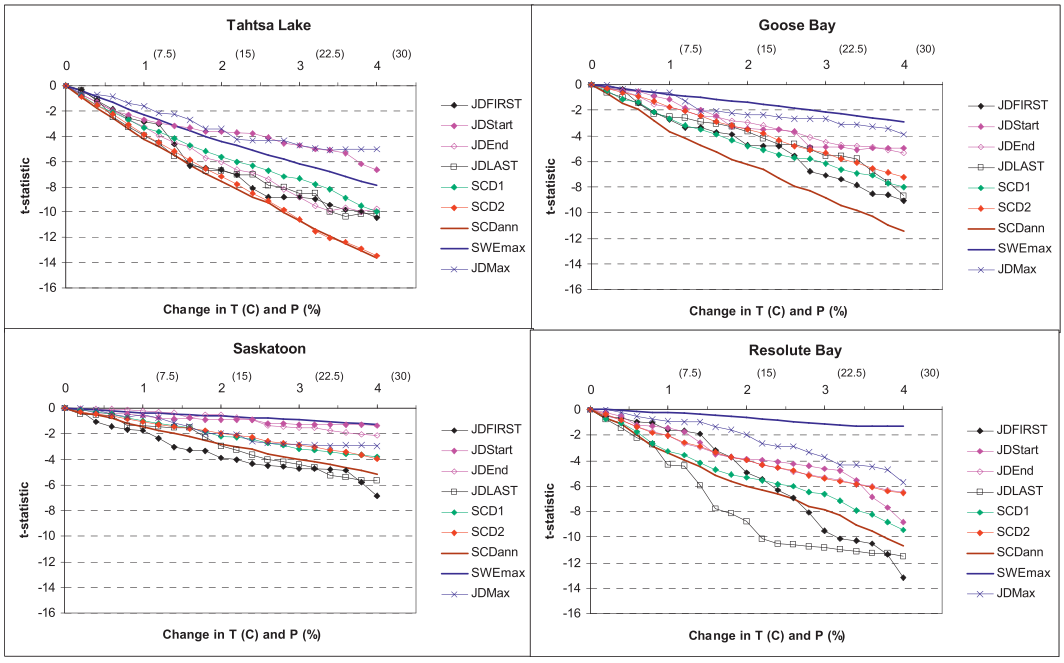


FIG. 6. Results of simulated snow cover response ($t$ statistic) to concurrent linear increases in temperature (+4°C) and precipitation (+30%): (top left) Tahsta Lake and (top right) Goose Bay. (bottom left) Saskatoon and (bottom right) Resolute Bay.

comparable to the maximum temperature sensitivity of 1 April SWE ($-200$ mm °C$^{-1}$) observed over lower elevations of the southern Sierra Nevada by Howat and Tulaczyk (2005). The zone of elevated SWE temperature sensitivity is caused by the combined effects of changes in snowfall amount and changes in the length of the snow cover season. At low elevations, the maximum SWE is limited by the shorter snow season, while at higher elevations the snow cover is continuous, so SWEmax can only respond to changes in snowfall amount. In the intermediate zone, SWEmax is influenced by both changing season length and the changes in snowfall amount. These results are consistent with snow cover duration temperature sensitivity results from the European Alps (Hantel et al. 2000; Hantel and Hirtl-Wielke 2007) and Scotland (Mandar et al. 2007), which show a zone of maximum SCD temperature sensitivity of approximately $-30$ days °C$^{-1}$ in a midelevation band between ~500 and 900 m. Figure 7 also suggests that warming and increasing precipitation may be associated with trends of opposite sign in SCD and SWEmax at some mid-elevation zone $\sim\Delta Z$ = 1000–1500 m, which may complicate the interpretation of the response of snow cover to warming in mountain regions. Analysis of published snow trends with respect to temperature as a proxy for elevation (Fig. 8) confirms the sensitivity study findings of stronger decreasing trends at lower elevations and in regions with more temperate winter climates.

In summary, the sensitivity analysis has provided the following guidance on possible twentieth-century changes in snow cover in response to a warming and a concomitant increase in precipitation:

- The snow variables likely to provide the largest climate change response across a range of snow-climate regimes are snow cover duration (SCDann, SCD1, and SCD2) and the first (JDfirst) and last (JDlast) dates of snow on the ground.
- The first evidence of a snow warming signal is most likely to be found over lower elevations of maritime and mountain snow-climate regions, that is, regions of high SWE with mild winter temperatures and in the *tundra* snow-climate region. In the latter region, the strongest signal is associated with the last date of snow on the ground, while in the former, annual snow cover duration has the strongest signal. These changes will be reinforced by albedo feedbacks in the spring period.
- The elevation response of snow cover and SWE varies with climate region, involves nonlinear interactions between snow cover duration and accumulated snowfall, and also depends on local factors, such as lapse rates, topography, and vegetation cover; these influences will complicate the interpretation of snow cover changes, particularly in mountain regions. The strongest elevation sensitivity of snow cover to

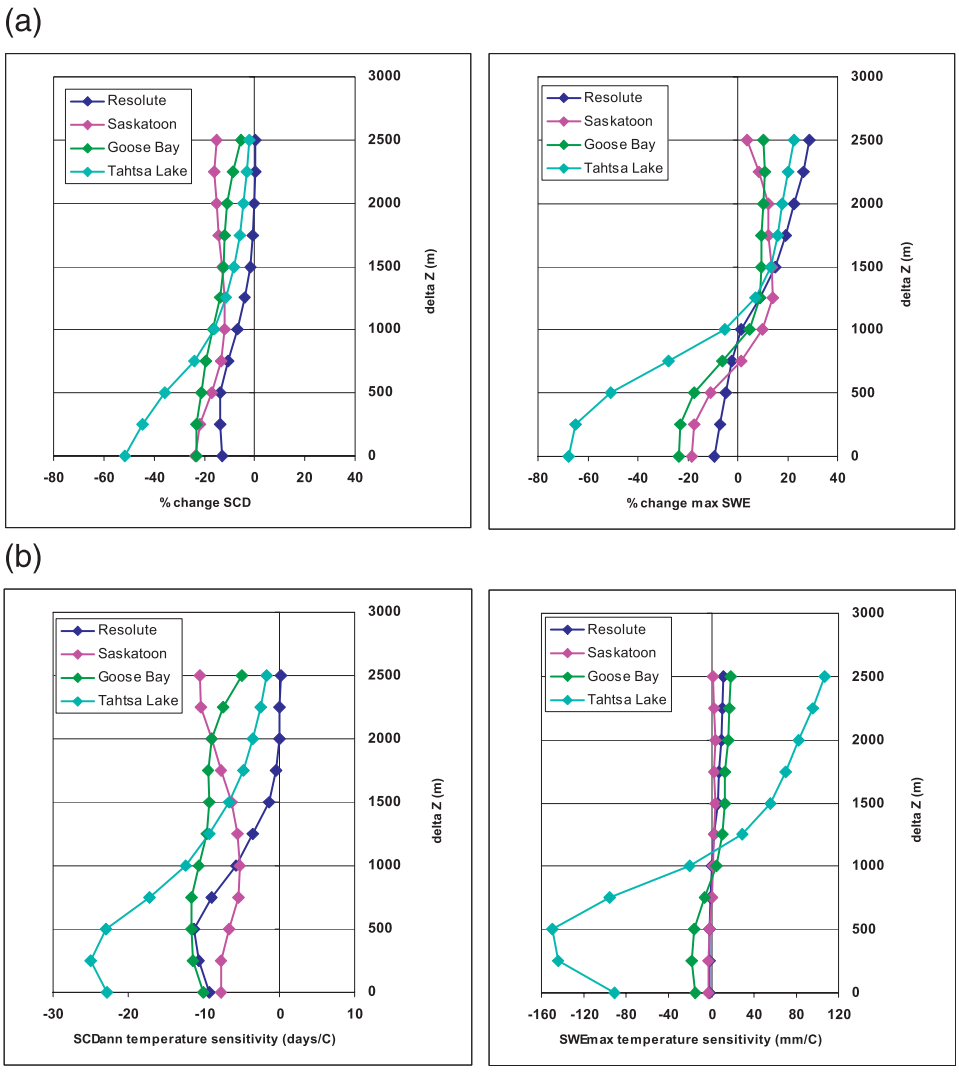


FIG. 7. (top left) Simulated change in SCDann and (top right) SWEmax at the four sites in response to a warming of 4°C and an increase in precipitation of 30%. (bottom left) SCDann and (bottom right) SWEmax temperature sensitivity.

climate change is most likely to be found in maritime climate regions.

- Significant reductions in SWEmax are most likely to be observed in maritime snow-climate regions and at lower elevations; significant increases in SWEmax are only likely to be observed at higher elevations where increases in SWEmax are not offset by decreases in snow season length.
- In mountainous regions, the response of SWEmax and SCD to warming temperature and increasing precipitation may fall into one of three regimes—(i) −SWEmax, −SCD; (ii) +SWEmax, −SCD; or (iii) +SWEmax, +SCD—depending on elevation, which can complicate the interpretation of snow cover trends.
- Increasing precipitation has a relatively small effect on the warming response of snow cover duration variables, but it does play an important role in offsetting reductions in SWEmax.
- JDmax may be a useful variable for climate monitoring, as it has less noise than SWEmax.

### *b. Observed snow cover response to NH warming in the NOAA dataset*

The results of trend analysis for observed fall, spring, and annual snow cover duration during the 1966–2007 period are presented in Fig. 9. The most obvious feature is the pronounced seasonal contrast with fall SCD, characterized by increases over much of Eurasia and the

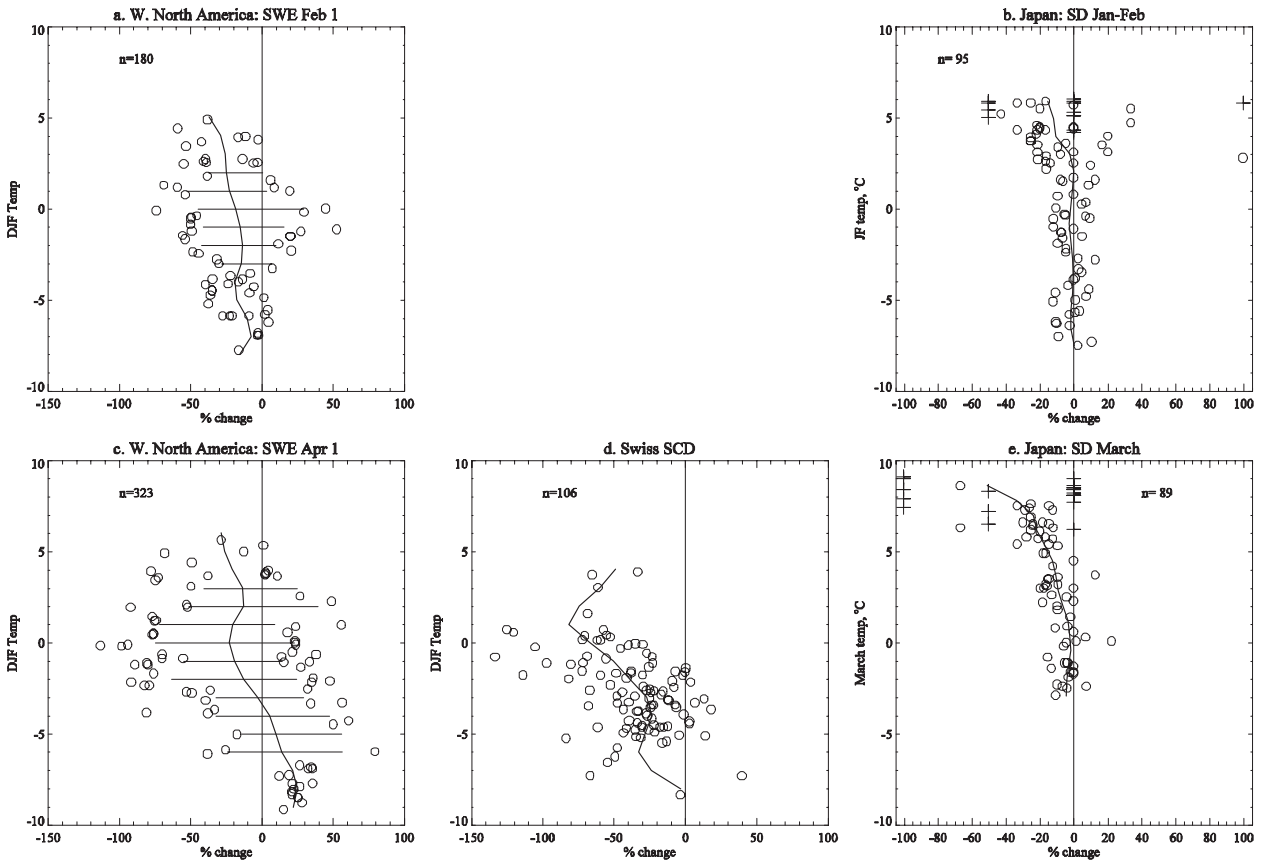


FIG. 8. Dependence of trends in measures of snow on site temperature. The number of data points is given in each panel. (a) Trends in 1 Feb SWE at mountain sites in western NA for 1950–2000. Smooth curve denotes the mean for each 1°C bin, and horizontal lines indicate the 5%–95% range for each bin. Circles show individual snow courses with trends outside that range. (b) Differences in average January–February SD at weather stations in Japan, 1960s minus 1990s. Sites with mean SD more than 2 cm are shown as circles and are used in computing the smooth curves shown; other sites are shown with pluses. (c) Same as (a), but for April. (d) Trends in snow cover duration (December–February) in Switzerland during the period of record 1958–99. (e) Same as (b), but for March. (a),(b) Show quantities and times of year that are less sensitive to temperature than those in (c)–(e).

interior of NA, while spring SCD is characterized by decreases over most NH land areas. Analysis of temperature trends in the CRUtem3v dataset and the National Centers for Environmental Prediction (NCEP) reanalysis (Kalnay et al. 1996) during the same period (not shown) indicate this different response is related to a slight cooling of temperatures in October–November over Alaska and central Canada, eastern Europe, and northern Siberia. In contrast, spring is characterized by a much stronger and widespread warming. The snow model sensitivity analysis for temperature decreases (not shown) indicated that a cooling on the order of 0.5°–1.0°C was sufficient to generate significant earlier onset of continuous snow cover (JDstart) at three of the climate stations (TL, RB, and GB). This effect is enhanced under increasing precipitation—for example, a cooling of only −0.3°C is required to generate a significant earlier onset to the continuous snow cover season at TL, with an increase in precipitation of 10%. We argue, therefore, that increasing precipitation (Zhang et al. 2007; Min et al. 2008) and the different temperature trends between early winter and spring periods are responsible for the asymmetric snow cover response observed in Fig. 9. This is consistent with observed significant increases in early winter SCE and SWE over the midlatitudes of North America during much of the twentieth century (Brown 2000).

The strongest decreases in spring snow cover extent are observed around the coastal margins of NA, Scandinavia, northern Russia, and over the Himalayas. This follows the findings of the sensitivity analysis results, which indicated that snow cover in areas with larger precipitation amounts were likely to be more sensitive to warming. To investigate this further, an analysis was made of ''at risk'' snow cover following Nolin and Daly (2006) by constructing a map of snow cover temperature

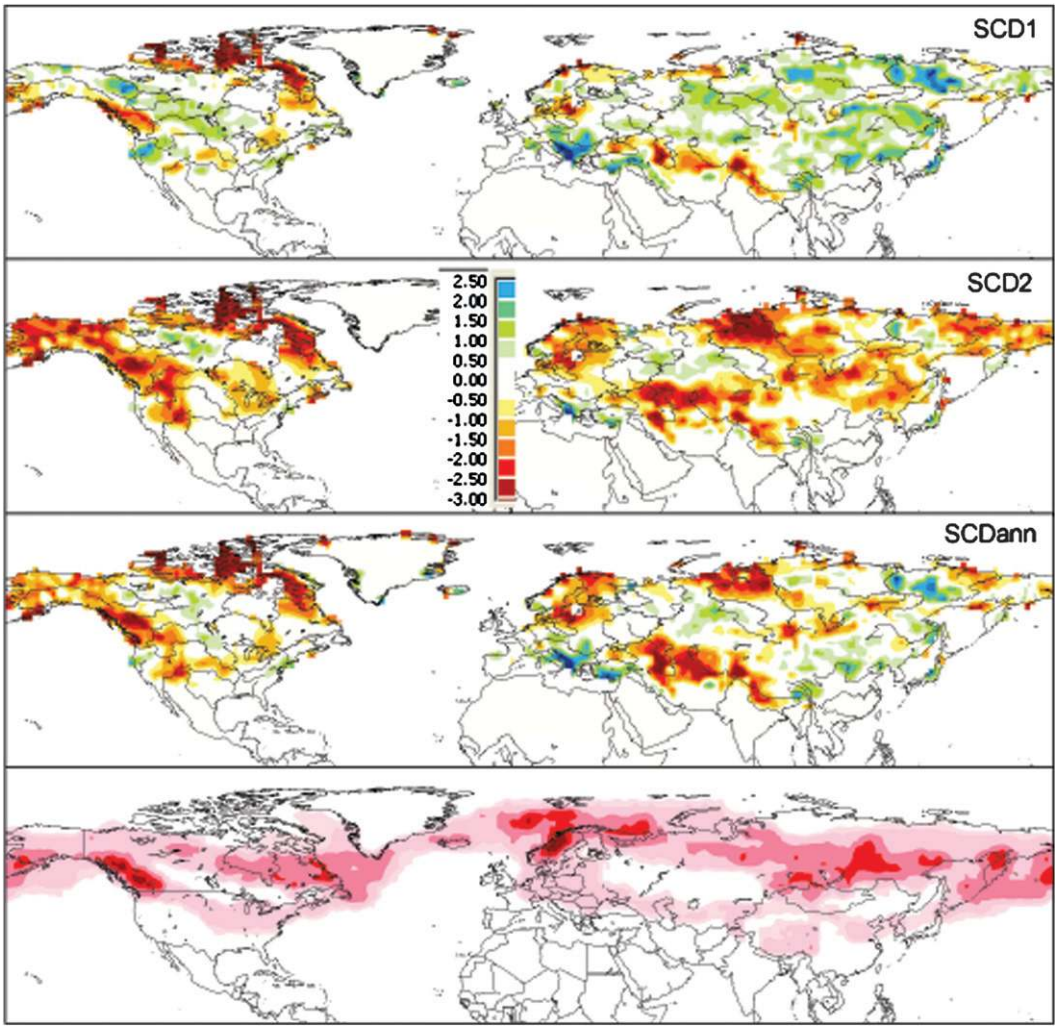


FIG. 9. (top three panels) Local $Z$ statistic for trend in snow cover duration during 1966–2007 from the NOAA weekly snow cover dataset for the fall, spring, and snow year. (bottom) Location of the zone where snow cover should be most sensitive to temperature based on temperature and precipitation climatology from the NCEP reanalysis (the darker the red, the longer the period of snow sensitivity).

change potential from mean monthly surface air temperature and precipitation rate in the NCEP reanalysis for the 1961–90 period. The classification scheme assigned a 0–3 sensitivity ranking based on an air temperature range of +5° to −5°C and mean precipitation amounts: 0—seasonal mean air temperatures warmer than +5° or colder than −5°C; 1—seasonal mean air temperatures in the range +5° to −5°C and the mean precipitation rate of <1 mm day$^{-1}$; 2—seasonal mean temperatures in the range +5° to −5°C and mean precipitation rate of 1–2 mm day$^{-1}$; and 3—seasonal mean temperature in the range +5°C to −5°C and mean precipitation rates >2 mm day$^{-1}$. The temperature range was selected based on analysis of observed snow cover changes in the NOAA dataset and corresponding mean temperatures from the NCEP reanalysis, while the precipitation thresholds are based on the observed range of mean precipitation values in the NCEP reanalysis.

The classification was carried out separately for the fall [September–November (SON)], winter [December–February (DJF)] and spring [April–June (AMJ)] periods, and the seasonal ranks added to provide an index of the amount of time a potential snow cover was in the temperature sensitive regime (Fig. 9, bottom). This temperature- and precipitation-based classification shows good qualitative agreement with the spatial pattern of observed change and correctly replicates the areas showing little change over the interior of both continents. This is consistent with the sensitivity analysis,

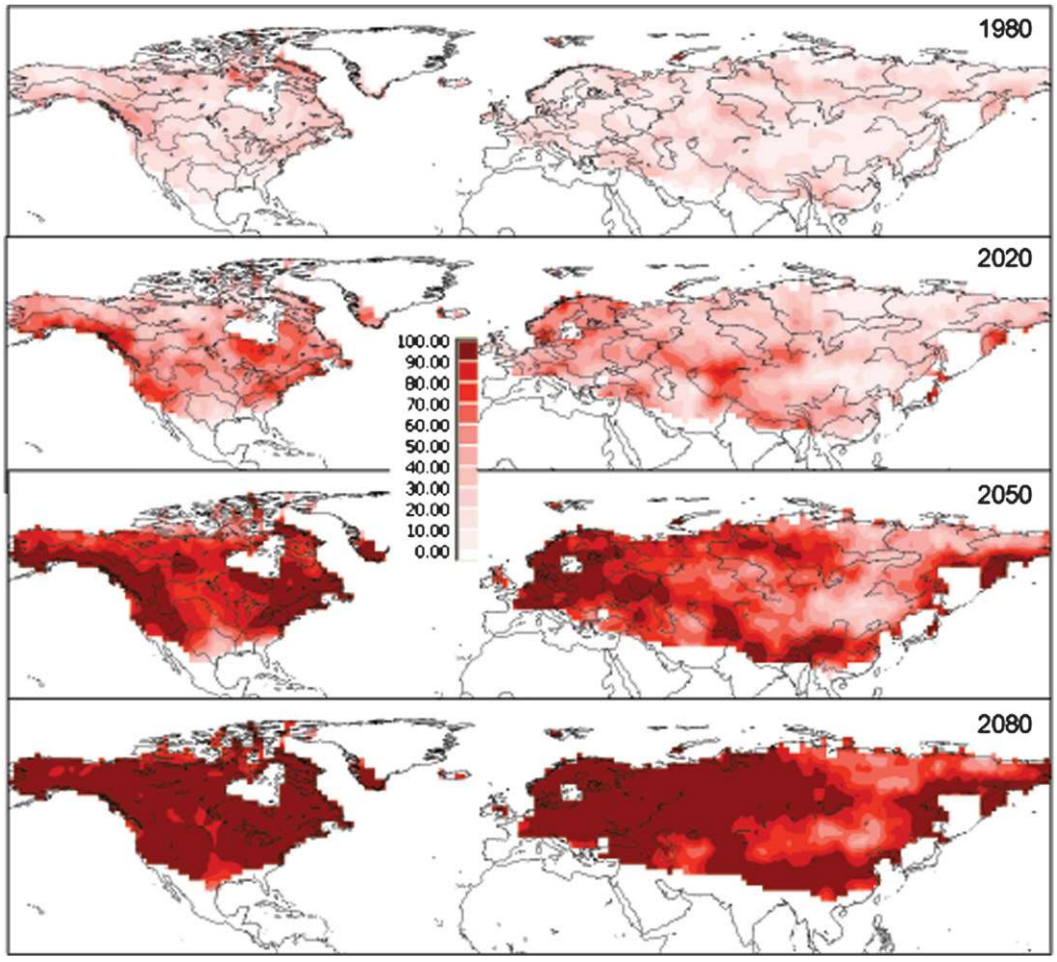


FIG. 10. Evolution of the climate warming signal in annual SCD from eight GCMs (% of models showing significant decreases). (top) Results are for 1970–99 vs 1900–29 from 20C3M simulations. (lower three panels) Results are computed from the A2 scenario with respect to a 1970–99 reference: 2020–2080. There is no model consensus for significant increases in SCDann.

which suggested the prairie snow cover climate regime has a much lower signal-to-noise ratio than other snow climate regions.

### c. *Simulated snow cover response to climate change in climate models*

The time sequence of changes in SCDann and SWEmax simulated by the CMIP3 models is shown in Figs. 10–12 as the percentage of models showing a statistically significant change. For SCDann, model consensus results are only presented for *decreasing* snow cover duration, as there was no model consensus for *increasing* snow cover. Hardly any models show significant decreases in SCDann (Fig. 10) during the twentieth century, except over the eastern Canadian Arctic and in British Columbia, but by 2020 a majority of models show significant decreases in snow cover over NA in two broad zones located over the western cordillera and east of ~90°W. The 2020 model consensus is more regional in character over Eurasia, with the main regions of consensus located over Scandinavia and Kazakhstan. By 2050 all models are showing significant decreases in SCD over the west and east coast regions of NA, while in Eurasia all models are indicating significant decreases over Europe and around the southern and eastern edges of the continental snow cover. The other feature that emerges in 2050 is the large zone of lower model consensus for significant SCD decreases over much of eastern Eurasia (east of ~90°E), which persists into 2080. In this region, the models show either no consensus (particular to grid points located over the eastern Tibetan Plateau) or a consensus for no significant change in SCD. The former may reflect difficulties representing complex terrain in GCMs (Cui et al. 2007),

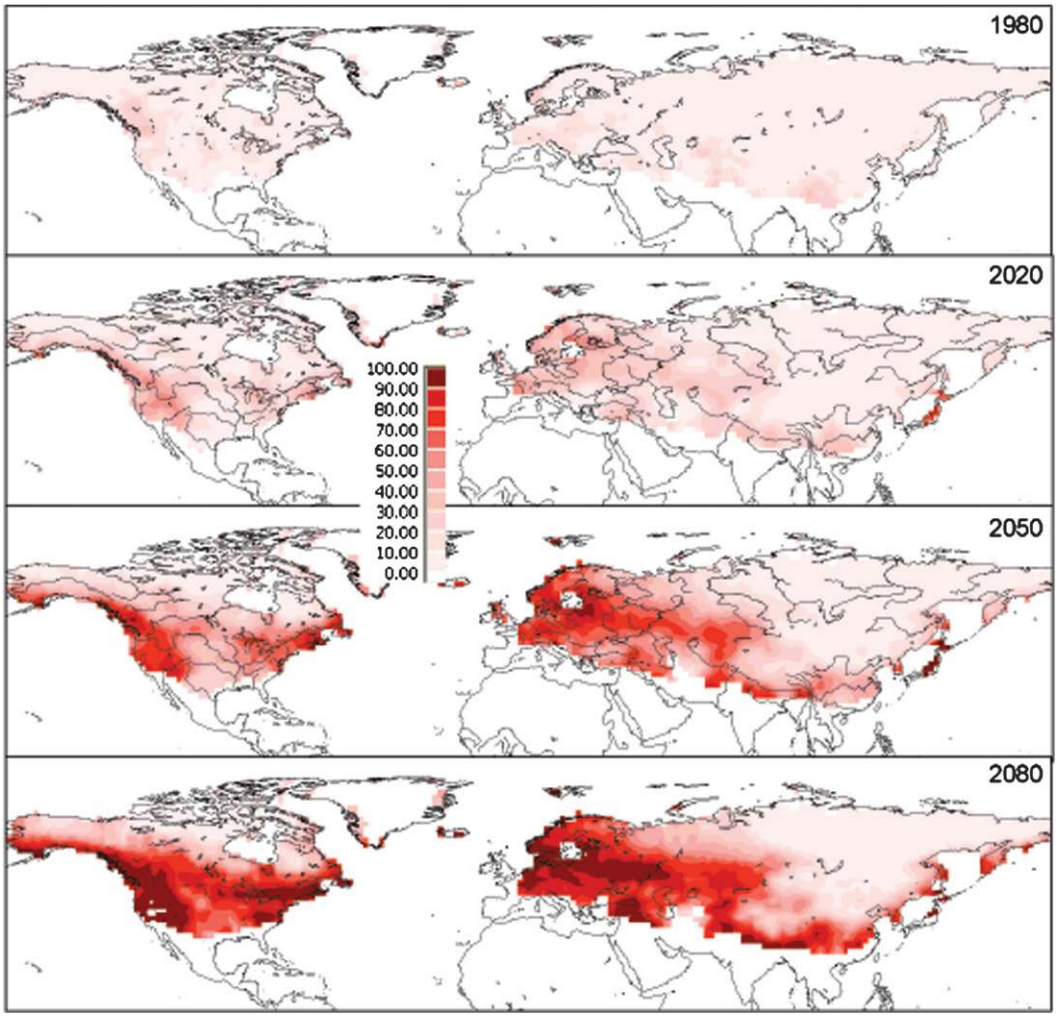


FIG. 11. Model consensus for significant decreases in SWEmax (% of 14 models). See Fig. 10 for definition of panels.

while the latter is likely linked to a slower snow cover change signal for dry continental locations, as seen in Saskatoon in Fig. 6.

The results for significant reductions in SWEmax (Fig. 11) do not show a clear model consensus until 2050, and the spatial domain of areas experiencing significant decreases in SWEmax is more constrained than SCD, with decreases mainly confined to midlatitudinal coastal regions of NA and western Europe. Over northern Canada, eastern Eurasia, and northern Russia, there is no model consensus for decreasing SWE. as these are regions where the model consensus is for no significant change or significant increases in SWE (Fig. 12). The areas of model consensus for significant decreases and increases in SWE correspond approximately to the 0° and −20°C isotherms for November–May mean air temperature (Fig. 13) following Räisänen (2007). Between these two isotherms are large regions (e.g., northern China and the boreal forest zone over NA) where the models show a consensus for no significant changes in SWE. This is consistent with the incremental analog results in Fig. 6, which showed that SWEmax did not exhibit significant change at two of the sites (SK and RB) under a scenario of $T$ +4°C and $P$ +30%.

There is some empirical evidence supporting increasing SWE over northern Eurasia—for example, Hyvärinen (2003) found increases of snow depth in eastern and northern Finland but decreases in the south and west. Ye et al. (1998) reported increased snow accumulation over Siberia in the same region where the CMIP3 models project increases in SWE. This was confirmed more recently by Kitaev et al. (2005), who document a general increase in snow depth and snow cover from daily snow depth observations over northern Eurasia from 1936–2000, although their snow

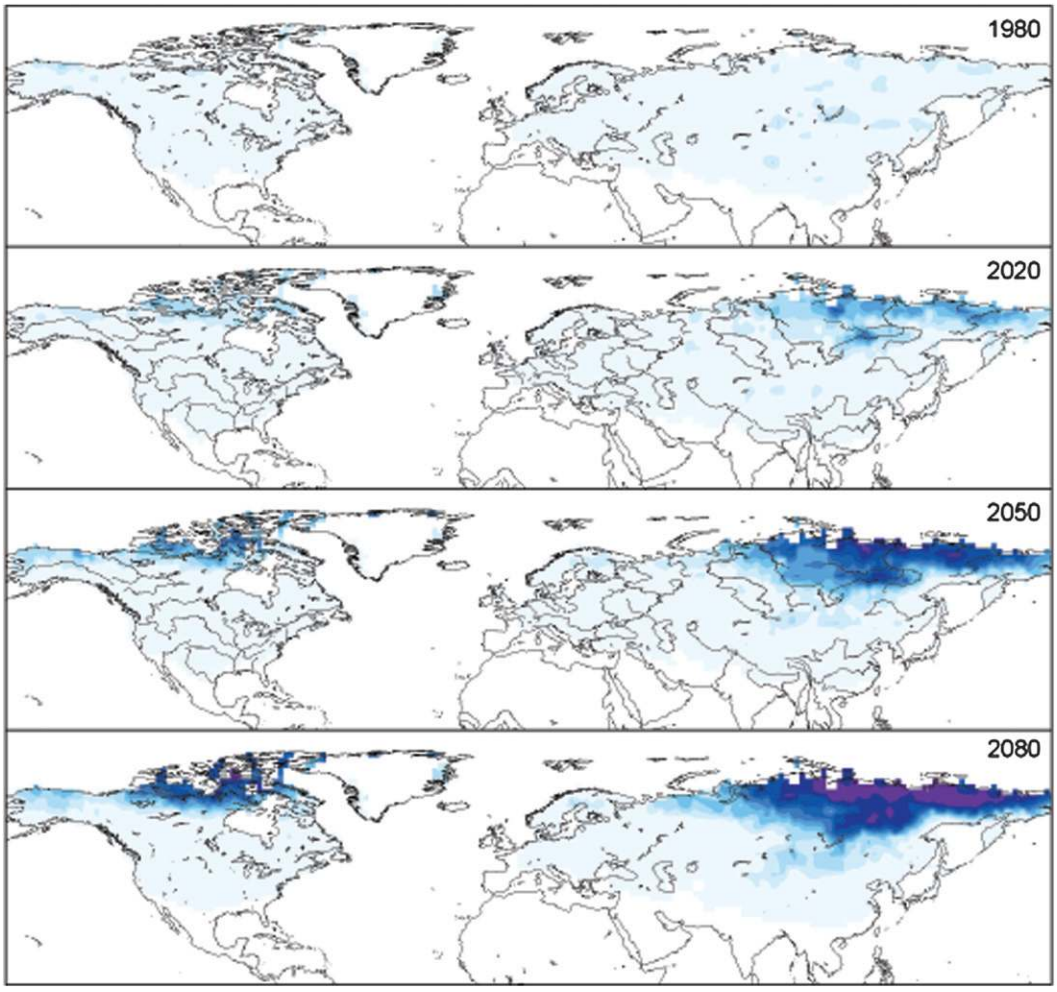


FIG. 12. Same as Fig. 11, but for significant increases in SWEmax (percent of 14 models showing significant increases).

cover duration time series suggest values peaked around the end of the 1970s then started a downward trend similar to twentieth-century trends in NA winter SCE documented by Brown (2000). This is consistent with the results of the sensitivity analysis, which showed that increasing SWE and decreasing SCD can exist for certain combinations of increasing temperature and precipitation (Fig. 7). The CMIP3 GCMs do not have sufficient resolution to capture the increase in SWE at higher elevations suggested by the sensitivity analysis, but this is apparent in dynamically downscaled SWE change scenarios (Fig. 14), which show increased SWE at higher elevations in the Rocky Mountains.

Overall, the model results are consistent with several aspects of the previous analyses. That is, they show an enhanced early response of snow cover to warming over the western cordillera of NA and maritime regions, such as eastern NA, Scandinavia, and the Pacific coast of Russia, and they indicate that snow cover changes are slower over continental interiors. The models are also consistent with the sensitivity analysis, in that they show an earlier consensus for significant reductions in snow cover before SWE (cf. Figs. 10 and 11). The areas where the models results are not consistent with observed trends and the sensitivity analysis are the lack of a consistent warming response over eastern Eurasia; the lack of clear evidence of earlier reductions in spring SCD over high latitudes, suggested from observed trends in SCD from the NOAA dataset and emerging evidence of accelerating reductions in snow cover over the Arctic spring–summer period (Déry and Brown 2007); and a circumpolar increase in maximum snow accumulation, which is not consistent with widespread reductions in winter snow depths over Canada since ~1950 (Brown and Braaten 1998; Kitaev et al. 2005; Derksen et al. 2007a). The first problem may be linked to difficulties simulating the climate interactions of the Tibetan Plateau in GCMs, and the second problem may be linked to

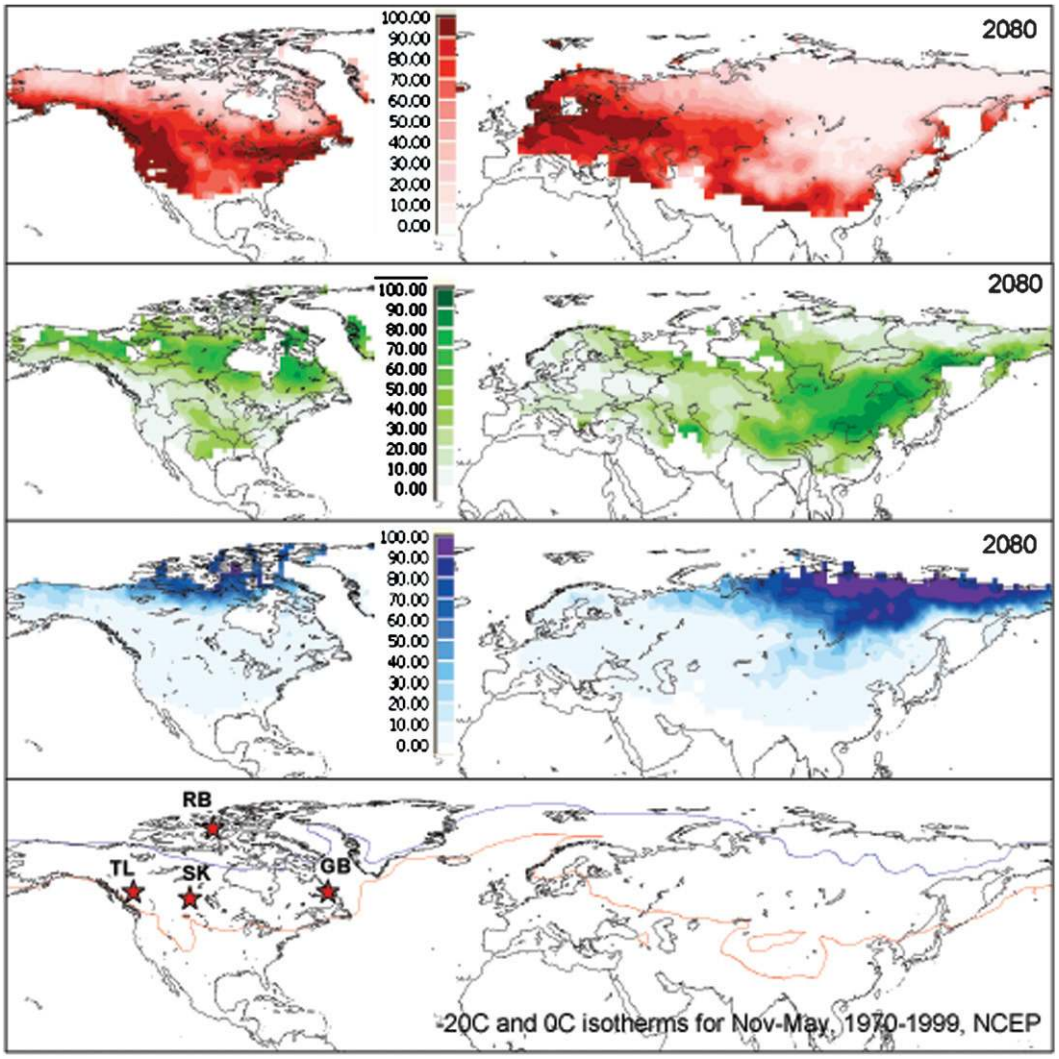


FIG. 13. Percent of 14 models showing (top to next to bottom panel) significant decreases, no increases, and significant increases in SWEmax between 2070–99 and 1970–99 compared to (bottom) the mean location of the November–May −20° (blue) and 0°C (red) isotherms; stars indicate the approximate locations of the four sites used in the sensitivity analysis.

inadequate treatment of snow processes. For example, Qu and Hall (2007) reported a large intermodel spread in snow–albedo feedback related to the treatment of vegetation.

## 5. Conclusions

The results of the analyses carried out in this paper suggest a complex response of NH snow cover to a climate change of increasing $T$ and $P$, with the strength (and signal-to-noise ratio) varying with climate regime, elevation, and snow cover variable. Snow cover duration was shown to have the strongest sensitivity to warming as measured by signal-to-noise ratio, with the largest relative changes in SCD and SWE over lower elevations of regions with a maritime winter climate—that is, moist climates with snow season temperatures in the range of −5° to +5°C. This corresponds to a midlatitudinal zone extending around the coastal margins of the continents, with snow cover in the drier, colder continental interior regions showing the lowest temperature sensitivity. Positive albedo feedbacks in the spring period generate a stronger signal in spring snow cover duration, with feedback potential increasing with latitude (Déry and Brown 2007).

The snow model sensitivity analysis suggested a potentially complex elevation response of SCD and SWEmax to increasing $T$ and $P$ in mountain regions as a result of nonlinear interactions between the duration of the snow season and snow accumulation rates. Joint

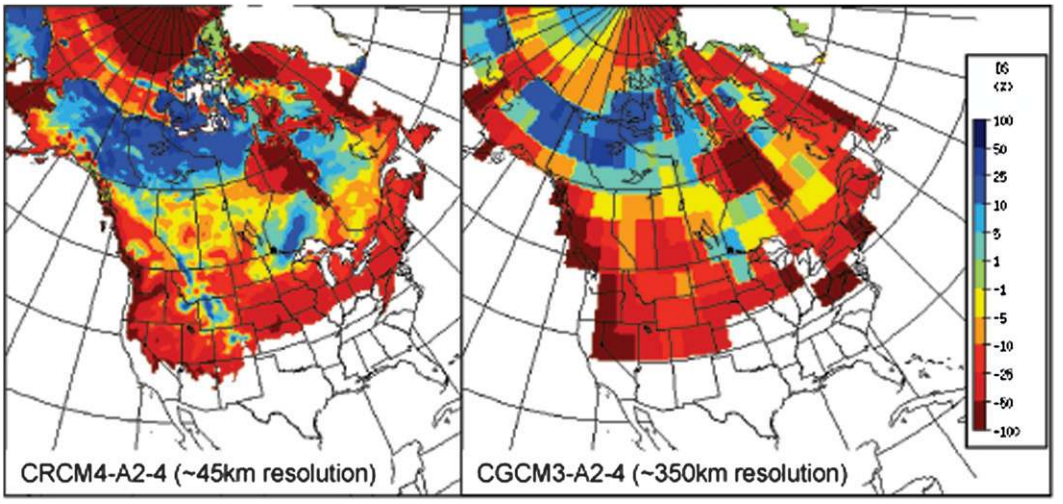


FIG. 14. Percent change in mean winter SWE between 1961–90 and 2041–70 for the Special Report on Emission Scenarios (SRES) A2 scenario. (left) Results from version 4.1.1 of the Canadian Regional Climate Model simulation (Music and Caya 2007) driven at its lateral boundaries by CGCM3 SRES A2 scenario, run4. (right) SWE change simulated by CGCM3 (source: Ouranos Climate Simulation Team).

response surface results of relative changes in SCD and SWEmax indicate three possible snow cover responses depending on the amount of warming and precipitation increase, the elevation, and the climate regime. Drier climate regimes were more likely to have a mixed response of increasing SWEmax and decreasing SCD, which may explain some of the variability in snow trends reported from western China. Local factors—such as lapse rate, aspect, topography, vegetation, and blowing snow transport—will further complicate the snow cover climate response in mountain regions.

Trends in snow cover duration observed from space during the 1966–2007 period are consistent with the spatial pattern of significant snow cover reduction simulated by the CMIP3 climate models, which show an early warming response of snow cover over the western cordillera of NA and maritime regions, such as eastern NA, Scandinavia, and the Pacific coast of Russia. The observed trends and the climate models also agree that significant snow cover changes are slower over continental interiors (in agreement with the sensitivity analysis). The climate models are also consistent with the sensitivity analysis and observed trends in that they show significant widespread reductions in snow cover occurring *before* significant reductions in SWEmax.

Observations of increasing snow depths over northern Eurasia are consistent with climate model projections of increased SWEmax over northern high latitudes. However, there is little observational evidence of increasing SWE from northern Canada. The exception is northern Quebec, where there is some proxy evidence of increasing snowfall from reconstructed lake levels (Bégin 2000) and analysis of black spruce growth forms (Lavoie and Payette 1992). According to Payette et al. (2004), increased snowfall since 1957 was the main climatic driver for accelerated permafrost thawing in northern Quebec between 1957 and 2003. Further work is needed to document snow accumulation trends over northern latitudes, as the surface observing networks are inadequate for monitoring regionally averaged SWE. It may be possible to develop regional SWE estimates from passive microwave data using new algorithms being developed specifically for the tundra region (Derksen et al. 2005; Rees et al. 2006; Derksen et al. 2007b). Further work is also needed to evaluate and improve the representation of snow cover in global climate models—in particular, the apparent overestimation of snow accumulation over northern high latitudes and the muted model response of snow cover duration to climate forcing over high latitudes and eastern Eurasia.

*Acknowledgments.* The idea for this paper was developed while the coauthor was on sabbatical at the Ouranos climate change consortium in Montréal during July 2007, and he thanks Ouranos for its partial support for the sabbatical. Anne Frigon from the Ouranos Climate Simulation Team is acknowledged for providing the regional climate model snow simulation shown in Fig. 14. We also thank S. Scherrer, M. Ishizaki, and N. Petkova for sharing the data used to construct Fig. 1, and X. Zhang

and the three anonymous referees for their helpful comments on the draft manuscript. We acknowledge the modeling groups, the Program for Climate Model Diagnosis and Intercomparison (PCMDI), and the WCRP's Working Group on Coupled Modelling (WGCM) for their roles in making available the WCRP CMIP3 multimodel dataset. Support of this dataset is provided by the Office of Science, U.S. Department of Energy. This publication is partially funded by the Joint Institute for the Study of the Atmosphere and Ocean (JISAO) under NOAA Cooperative Agreement NA17RJ1232.

## REFERENCES

Anderson, E. A., 1973: National Weather Service River Forecast System—Snow accumulation and ablation model. NOAA Tech. Memo. NWS Hydro-17, 217 pp.

Bales, R. C., N. P. Molotch, T. H. Painter, M. D. Dettinger, R. Rice, and J. Dozier, 2006: Mountain hydrology of the western United States. *Water Resour. Res.,* **42,** W08432, doi:10.1029/2005WR004387.

Barnett, T. P., and Coauthors, 2008: Human-induced changes in the hydrology of the western United States. *Science,* **319,** 1080–1083, doi:10.1126/science.1152538.

Barry, R. G., 1984: Possible $CO_2$-induced warming effects on the cryosphere. *Climatic Changes on a Yearly to Millennial Basis*, N.-A. Mörner and W. Karlén, Eds., D. Reidel, 571–604.

Bégin, Y., 2000: Reconstruction of subarctic lake levels over past centuries using tree rings. *J. Cold Reg. Eng.,* **14,** 192–212.

Brasnett, B., 1999: A global analysis of snow depth for numerical weather prediction. *J. Appl. Meteor.,* **38,** 726–740.

Brohan, P., J. J. Kennedy, I. Harris, S. F. B. Tett, and P. D. Jones, 2006: Uncertainty estimates in regional and global observed temperature changes: A new data set from 1850. *J. Geophys. Res.,* **111,** D12106, doi:10.1029/2005JD006548.

Brown, R. D., 2000: Northern Hemisphere snow cover variability and change, 1915–97. *J. Climate,* **13,** 2339–2355.

——, and R. O. Braaten, 1998: Spatial and temporal variability of Canadian monthly snow depths, 1946-1995. *Atmos.–Ocean,* **36,** 37–45.

——, and A. Frei, 2007: Comment on ''Evaluation of surface albedo and snow cover in AR4 coupled models'' by A. Roesch. *J. Geophys. Res.,* **112,** D22102, doi:10.1029/2006JD008339.

——, and N. Petkova, 2007: Snow cover variability in Bulgarian mountainous regions, 1931-2000. *Int. J. Climatol.,* **27,** 1215–1229.

——, B. Brasnett, and D. Robinson, 2003: Gridded North American monthly snow depth and snow water equivalent for GCM evaluation. *Atmos.–Ocean,* **41,** 1–14.

——, C. Derksen, and L. Wang, 2007: Assessment of spring snow cover duration variability over northern Canada from satellite datasets. *Remote Sens. Environ.,* **111,** 367–381.

Changchun, X., C. Yaning, L. Weihong, C. Yapeng, and G. Hongtao, 2007: Potential impact of climate change on snow cover area in the Tarim River basin. *Environ. Geol.,* **53,** 1465–1474.

Christensen, J. H., and Coauthors, 2007: Regional climate projections. *Climate Change 2007: The Physical Science Basis.* S. Solomon et al., Eds., Cambridge University Press, 847–940.

Cui, X., B. Langmann, and H.-F. Graf, 2007: Summer monsoonal rainfall simulation on the Tibetan Plateau with a regional climate model using a one-way double-nesting system. *SOLA,* **3,** 49–52, doi:10.2151/sola.2007-013.

Derksen, C., A. Walker, and B. Goodison, 2005: Evaluation of passive microwave snow water equivalent retrievals across the boreal forest/tundra transition of western Canada. *Remote Sens. Environ.,* **96,** 315–327.

——, R. Brown, and M. MacKay, 2007a: Mackenzie Basin snow cover: Variability and trends from conventional data, satellite remote sensing, and Canadian regional climate model simulations. *Atmospheric Dynamic*s, M.-K. Woo, Ed., Vol. 1, *Cold Region Atmospheric and Hydrologic Studies: The Mackenzie GEWEX Experience,* Springer-Verlag, 213–240.

——, A. Walker, and P. Toose, 2007b: Estimating snow water equivalent in northern regions from satellite passive microwave data. *Atmospheric Dynamics,* M.-K. Woo, Ed., Vol. 1, *Cold Region Atmospheric and Hydrologic Studies: The Mackenzie GEWEX Experience.* Springer-Verlag, 195–212.

Déry, S. J., and R. D. Brown, 2007: Recent Northern Hemisphere snow cover extent trends and implications for the snow-albedo feedback. *Geophys. Res. Lett.,* **34,** L22504, doi:10.1029/2007GL031474.

Falarz, M., 2004: Variability and trends in the duration and depth of snow cover in Poland in the 20th century. *Int. J. Climatol.,* **20,** 1723–1727.

Foster, D. J., Jr., and R. D. Davy, 1988: Global snow depth climatology. USAF Environmental Technical Applications Center Rep. USAFETAC/TN-88/006, 48 pp.

Foster, J., and Coauthors, 1996: Snow cover and snow mass intercomparisons of general circulation models and remotely sensed datasets. *J. Climate,* **9,** 409–426.

Frei, A., and D. A. Robinson, 1998: Evaluation of snow extent and its variability in the Atmospheric Model Intercomparison Project. *J. Geophys. Res.,* **103,** 8859–8871.

——, and G. Gong, 2005: Decadal to century scale trends in North American snow extent in coupled atmosphere–ocean general circulation models. *Geophys. Res. Lett.,* **32,** L18502, doi:10.1029/2005GL023394.

——, J. A. Miller, and D. A. Robinson, 2003: Improved simulations of snow extent in the second phase of the Atmospheric Model Intercomparison Project (AMIP-2). *J. Geophys. Res.,* **108,** 4369, doi:10.1029/2002JD003030.

——, R. Brown, J. A. Miller, and D. A. Robinson, 2005: Snow mass over North America: Observations and results from the second phase of the Atmospheric Model Intercomparison Project (AMIP-2). *J. Hydrometeor.,* **6,** 681–695.

Fyfe, J. C., and G. M. Flato, 1999: Enhanced climate change and its detection over the Rocky Mountains. *J. Climate,* **12,** 230–243.

Giorgi, F., J. W. Hurrell, M. R. Marinucci, and M. Beniston, 1997: Elevation signal in surface climate change: A model study. *J. Climate,* **10,** 288–296.

Goodison, B., and A. E. Walker, 1993: Data needs for detection of climate change: Some challenges. NOAA Glaciological Data Report GD-25, 241–253.

Groisman, P. Ya., T. R. Karl, and R. R. Heim Jr., 1993: Inferences of the North American snowfall and snow cover with recent global temperature changes. NOAA Glaciological Data Rep. GD-25, 44–51.

——, ——, and R. W. Knight, 1994: Observed impact of snow cover on the heat balance and the rise of continental spring temperatures. *Science,* **263,** 198–200.

Hamlet, A. F., P. W. Mote, M. P. Clark, and D. P. Lettenmaier, 2005: Effects of temperature and precipitation variability on snowpack trends in the western United States. *J. Climate,* **18,** 4545–4561.

Hantel, M., and L.-M. Hirtl-Wielke, 2007: Sensitivity of Alpine snow cover to European temperature. *Int. J. Climatol.,* **27,** 1265–1275.

——, M. Ehrendorfer, and A. Haslinger, 2000: Climate sensitivity of snow cover duration in Austria. *Int. J. Climatol.,* **20,** 615–640.

Hennessy, K., P. Whetton, I. Smith, J. Bathols, M. Hutchinson, and J. Sharples, 2003: The impact of climate change on snow conditions in mainland Australia. CSIRO Atmospheric Research, 47 pp. [Available online at http://www.cmar.csiro.au/e-print/open/hennessy_2003a.pdf.]

Howat, I. M., and S. Tulaczyk, 2005: Climate sensitivity of spring snowpack in the Sierra Nevada. *J. Geophys. Res.,* **110,** F04021, doi:10.1029/2005JF000356.

Hyvärinen, V., 2003: Trends and characteristics of hydrological time series in Finland. *Nord. Hydrol.,* **34,** 71–90.

Ishizaka, M., 2004: Climatic response of snow depth to recent warmer winter seasons in heavy-snowfall areas in Japan. *Ann. Glaciol.,* **38,** 299–304.

Kalnay, E., and Coauthors, 1996: The NCEP/NCAR 40-Year Reanalysis Project. *Bull. Amer. Meteor. Soc.,* **77,** 437–471.

Kitaev, L., E. Førland, V. Razuvaev, O. E. Tveito, and O. Krueger, 2005: Distribution of snow cover over northern Eurasia. *Nord. Hydrol.,* **36,** 311–319.

Knowles, N., M. D. Dettinger, and D. R. Cayan, 2006: Trends in snowfall versus rainfall for the western United States. *J. Climate,* **19,** 4545–4554.

Kuusisto, E., 1980: On the values and variability of degree-day melting factor in Finland. *Nord. Hydrol.,* **11,** 235–242.

——, 1984: *Snow Accumulation and Snowmelt in Finland*. No. 55, *Publications of the Water Research Institute,* National Board of Waters, Finland, 149 pp.

Laternser, M., and M. Schneebeli, 2003: Long-term snow climate trends of the Swiss Alps (1931–99). *Int. J. Climatol.,* **23,** 733–750.

Lavoie, C., and S. Payette, 1992: Black spruce growth as a record of a changing winter environment at treeline, Québec, Canada. *Arct. Alp. Res.,* **25,** 40–49.

Lemke, P., and Coauthors, 2007: Observations: Changes in snow, ice and frozen ground. *Climate Change 2007: The Physical Science Basis.* S. Solomon et al., Eds, Cambridge University Press, 337–383.

Li, X., and Coauthors, 2008: Cryospheric change in China. *Global Planet. Change,* **62,** 210–218.

Liston, G. E., and M. Sturm, 1998: Global seasonal snow classification system. National Snow and Ice Data Center, Boulder, CO, digital media. [Available online at http://www.nsidc.org/data/arcss045.html.]

Mandar, R., M. K. Browne, P. M. Berry, T. P. Dawson, and M. D. Morecroft, 2007: Projecting climate change impacts on mountain snow cover in central Scotland from historical patterns. *Arct. Antarct. Alp. Res.,* **39,** 488–499.

Marshall, S. J., M. J. Sharp, D. O. Burgess, and F. S. Anslow, 2007: Near-surface-temperature lapse rates on the Prince of Wales Icefield, Ellesmere Island, Canada: Implications for regional downscaling of temperature. *Int. J. Climatol.,* **27,** 385–398.

Masiokas, M. H., R. Villalba, B. H. Luckman, C. Le Quesne, and J. C. Aravena, 2006: Snowpack variations in the Central Andes of Argentina and Chile, 1951–2005: Large-scale atmospheric influences and implications for water resources in the region. *J. Climate,* **19,** 6334–6352.

Mearns, L. O., M. Hulme, T. R. Carter, R. Leemans, M. Lal, and P. H. Whetton, 2001: Climate scenario development. *Climate Change 2001: The Scientific Basis*. J. T. Houghton et al., Eds., Cambridge University Press, 739–768.

Meehl, G. A., C. Covey, T. Delworth, M. Latif, B. McAvaney, J. F. B. Mitchell, R. J. Stouffer, and K. E. Taylor, 2007: The WCRP CMIP3 multimodel dataset: A new era in climate change research. *Bull. Amer. Meteor. Soc.,* **88,** 1383–1394.

Meteorological Service of Canada, 2000: *Canadian Snow Data*. CRYSYS Project, Climate Processes and Earth Observation Division, Meteorological Service of Canada, CD-ROM [Available online at http://ccin.ca.]

Min, S.-K., X. Zhang, and F. Zwiers, 2008: Human-induced Arctic moistening. *Science,* **320,** 518–520.

Mote, P. W., 2006: Climate-driven variability and trends in mountain snowpack in western North America. *J. Climate,* **19,** 6209–6220.

——, A. F. Hamlet, M. P. Clark, and D. P. Lettenmaier, 2005: Declining mountain snowpack in western North America. *Bull. Amer. Meteor. Soc.,* **86,** 39–49.

Music, B., and D. Caya, 2007: Evaluation of the hydrological cycle over the Mississippi River basin as simulated by the Canadian Regional Climate Model (CRCM). *J. Hydrometeor.,* **8,** 969–988.

Nolin, A. W., and C. Daly, 2006: Mapping ''at risk'' snow in the Pacific Northwest. *J. Hydrometeor.,* **7,** 1164–1171.

Payette, S., A. Delwaide, M. Caccianiga, and M. Beauchemin, 2004: Accelerated thawing of subarctic peatland permafrost over the last 50 years. *Geophys. Res. Lett.,* **31,** 18208, doi:10.1029/2004GL020358.

Pomeroy, J. W., and D. M. Gray, 1995: Snowcover accumulation relocation and management. National Hydrology Research Institute Science Rep. 7, 144 pp.

Popova, V., 2007: Winter snow depth variability over northern Eurasia in relation to recent atmospheric circulation changes. *Int. J. Climatol.,* **27,** 1721–1733.

Qin, D., S. Liu, and P. Li, 2006: Snow cover distribution, variability, and response to climate change in western China. *J. Climate,* **19,** 1820–1833.

Qu, X., and A. Hall, 2007: Assessing snow albedo feedback in simulated climate change. *J. Climate,* **19,** 2617–2630.

Räisänen, J., 2007: Warmer climate: Less or more snow? *Climate Dyn.,* **30,** 307–319, doi:10.1007/s00382-007-0289-y.

Ramsay, B., 1998: The interactive multisensor snow and ice mapping system. *Hydrol. Processes,* **12,** 1537–1546.

Randall, D. A., and Coauthors, 2007: Climate models and their evaluation. *Climate Change 2007: The Physical Science Basis.* S. Solomon et al., Eds., Cambridge University Press, 589–662.

Rees, A., C. Derksen, M. English, A. Walker, and C. Duguay, 2006: Uncertainty in snow mass retrievals from satellite passive microwave data in lake-rich high-latitude environments. *Hydrol. Processes,* **20,** 1019–1022.

Regonda, S. K., B. Rajagopalan, M. Clark, and J. Pitlick, 2005: Seasonal cycle shifts in hydroclimatology over the western United States. *J. Climate,* **18,** 372–384.

Robinson, D. A., 1993: Monitoring Northern Hemisphere snow cover. NOAA Glaciological Data Rep. GD-25, 1–25.

——, F. T. Keimig, and K. F. Dewey, 1991: Recent variations in Northern Hemisphere snow cover. *Proc. 15th NOAA Annual Climate Diagnostics Workshop,* Asheville, NC, National Oceanic and Atmospheric Administration, 219–224.

——, K. F. Dewey, and R. R. Heim, 1993: Global snow cover monitoring: An update. *Bull. Amer. Meteor. Soc.,* **74,** 1689–1696.

Roesch, A., 2006: Evaluation of surface albedo and snow cover in AR4 coupled climate models. *J. Geophys. Res.,* **111,** D15111, doi:10.1029/2005JD006473.

Scherrer, S. C., C. Appenzeller, and M. Laternser, 2004: Trends in Swiss alpine snow days: The role of local- and large-scale

climate variability. *Geophys. Res. Lett.,* **31,** L13215, doi:10.1029/2004GL020255.

Sen, P. K., 1968: Estimates of the regression coefficient based on Kendall's tau. *J. Amer. Stat. Assoc.,* **63,** 1379–1389.

Sturm, M., J. Holmgren, and G. E. Liston, 1995: A seasonal snow cover classification system for local to global applications. *J. Climate,* **8,** 1261–1283.

Vojtek, M., P. Faško, and P. Šťastný, 2003: Some selected snow climate trends in Slovakia with respect to altitude. *Acta Meteor. Univ. Comenianae,* **32,** 17–27.

Wang, L., M. Sharp, R. Brown, C. Derksen, and B. Rivard, 2005: Evaluation of spring snow covered area depletion in the Canadian Arctic from NOAA snow charts. *Remote Sens. Environ.,* **95,** 453–463.

Yang, J., Y. Ding, S. Liu, and J.-F. Liu, 2007: Variations of snow cover in the source regions of the Yangtse and Yellow Rivers in China between 1960 and 1999. *J. Glaciol.,* **53,** 420–426.

Ye, H., 2001: Increases in snow season length due to earlier first snow and later last snow dates over north central and northwest Asia during 1937–94. *Geophys. Res. Lett.,* **28,** 551–554.

——, H.-R. Cho, and P. E. Gustafson, 1998: The changes in Russian winter snow accumulation during 1936–83 and its spatial patterns. *J. Climate,* **11,** 856–863.

Zhang, G.-S., X.-H. Shi, D.-L. Li, Q.-C. Wang, and S. Dai, 2006: Climate change in Tuotuohe area at the headwaters of Yangtze River. *J. Glaciol. Geocryol.,* **28,** 678–685.

Zhang, X., L. A. Vincent, W. D. Hogg, and A. Niitsoo, 2000: Temperature and precipitation trends in Canada during the 20th century. *Atmos.–Ocean,* **38,** 395–429.

——, F. W. Zwiers, G. C. Hegerl, F. H. Lambert, N. P. Gillet, S. Solomon, P. A. Stott, and T. Nozawa, 2007: Detection of human influences on twentieth-century precipitation trends. *Nature,* **448,** 461–465, doi:10.1038/nature06025.

Zhao, H., and G. W. K. Moore, 2006: Reduction in Himalayan snow accumulation and weakening of the trade winds over the Pacific since the 1840s. *Geophys. Res. Lett.,* **33,** L17709, doi:10.1029/2006GL027339.